The authors are grateful to the time spent by Editor Maria Ana Baptista on monitoring the review process and by Prof. Mustafa Erdik (hereafter referred to as "RC1") and another anonymous reviewer (hereafter referred to as "RC2") on carefully reading our work and giving a series of constructive comments. All your efforts have greatly improved the manuscript. Point-to-point responses to reviewer comments are given as follows. The comments are in purple. Our responses are in blue. Accepted changes made in the revised manuscript are in green. The responses are followed by a marked-up version tracking all the changes we made in the revised manuscript. The authors are glad to respond to any of your further concern regarding this revised version.

Part 1: Comments from RC1 and our Responses and Changes in the revised manuscript.

(i) **General comments from RC1:** "The paper essentially aims the development of intensity-PGA relationships using a novel method that relies on comparison of intensity-based empirical and PGA-based analytical fragility relationships for the same building types from China. To fulfill this object, the authors first review the empirical building fragility database, mostly for China, scrutinize the data and derive the median Chinese intensity-based fragility relationships with basic treatment of uncertainties. For this empirical fragility study, three types of masonry buildings with different construction practices are considered. Secondly, the authors inspected publications that provide PGA-based analytical fragility functions (dependent on PGA) for the same damage classes and building categories. Thus, a solid fragility database and median fragility relationships, based on both intensity and PGA, are established for mainland China. For the derivation of median fragility relationships, the lognormal distribution is used with excellent goodness of fit. The paper culminates with the description and application of the novel approach for the development of the intensity-PGA relation by using fragility as the transfer medium. The results obtained are very valuable and compare well with limited relationships based on direct regression of measured PGA with the assessed intensity values."

(ii) Response: Thank you for this summarization and such positive judgement on our work.

(i) **RC1 comment 1:** "Very comprehensive literature review and description of ingredients and methodology on the assessment of fragility relationships from empirical data."

(ii) Response: Thank you for saying so.

(i) **RC1 comment 2:** "Text can be shortened since involves several repetitions of the objectives and methodologies."

(ii) Response: From the feedbacks of previous reviewing process, some reviewers misunderstood or partially neglected the focuses of this work. Therefore, although the objectives and methodologies are firstly mentioned in the Introduction section, to emphasize and to avoid possible misunderstanding from future readers, the focuses are thus reiterated in Section 4 and Section 5.2.

(iii) Changes in the revised manuscript: Accepted. The repetition in Section 4.2 is deleted.

(i) **RC1 comment 3:** "With the exception of the information provided on general approaches on the derivation of analytical vulnerabilities, not much detail is provided on the papers that the PGA-based analytical fragilities for the Chinese building stock. It appears that, with the exception of outlier removal, results on all these papers are given the same weight for the median fragility assessment. "

(ii) Response: The analytical fragility related studies for the Chinese building stock generally follow the classical methods and procedures as summarized in Page 4 Line27-36. Therefore, the details of these procedures are not presented in detail, since there is marginal exception.

You are right in that we do give the same weight for different intensity/PGA levels in regressing the median fragility curves, to avoid the introducing of extra subjective uncertainty. Since we noticed in previous literature, some researchers gave higher weight to lower intensity/PGA levels (e.g. Ding et al., 2017) in their regression, while others gave higher weight to higher intensity/PGA levels (e.g. Ma et al., 2014) with different focuses.

(i) **RC1 comment 4:** "The uncertainties in the fragility assessments are not adequately covered in the paper with the exception of uncertainties illustrated in Appendix Fig. A1-A4 and Table B1)."

(ii) Response: Thank you for pointing this out. RC2 also gives a detailed suggestion in regard of this. We'll accept the suggestions of you two and combine the error-bar analysis in the Appendix Fig. A1 and Fig. A2 with the median fragility curve in Fig. 7 and Fig. 8 in the main context, respectively.

(iii) Changes in the revised manuscript: Accepted. Fig. 7 and Fig. 8 are updated by integrating the error-bar analysis in Appendix Fig. A1 and Fig. A2, respectively. The original Fig. A1 and Fig. A2 are replaced by new figures, as explained below.

(i) **RC1 comment 5:** "Direct comparison of different fragility relationships is a difficult issue due to different building, damage state and ground motion intensity definitions and attributes considered in these relationships. This fact also manifests itself in this paper. Upon comparison of fragility relationships obtained in this paper with the results of several relevant international projects, only one (HAZUS Project) similarity for "Masonry – A" building type was found."

(ii) Response: Yes, this part was added to respond to the comments of one reviewer in the previous reviewing process. And we do notice the difficulty to conduct such comparison, given the difficulties as you summarized above. Actually, such a grand topic deserves individual deep-going study. Therefore, to keep the integrity and narrow down the focus of our current work, we'll remove the comparisons in Section 4.2 and delete the related descriptions in the main context and figures in the Appendix.

(iii) Changes in the revised manuscript: Section 4.2 and related descriptions in the context are removed. Figure A5, A6, A7 in the Appendix section are also deleted.

(i) **RC1 comment 6:** "The intensity-PGA relationships developed by using the correspondence between the empirical and PGA-based analytical fragility relationships is based on a novel approach and would be very valuable for use in international projects. However, a description on the relationship between the Chinese Official Seismic Intensity Scale (GB17742) and the other internationally adopted scales (e.g. MMI, MSK, EMS) may need to be included (or referenced) in the paper."

(ii) Response: Thank you for this suggestion. We found in previous studies (e.g. in Daniell, 2014) such work has been conducted. We'll add these references in the main context and add the following graphic comparison of different intensity scales into the Appendix.

(iii) Changes in the revised manuscript: The following Figure R1 is added into the Appendix as the new Figure A1. Related references are also added in the main context.

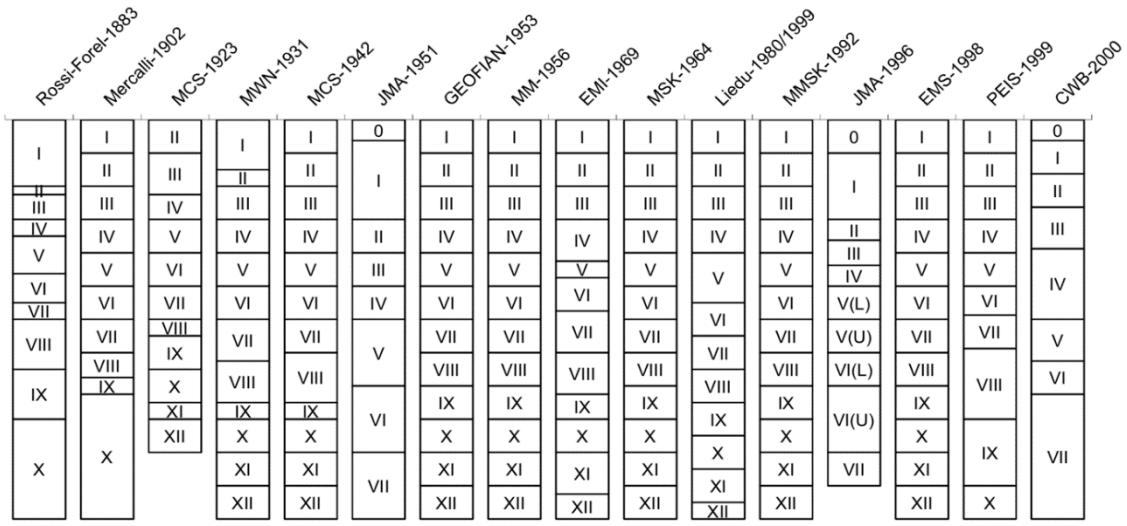

Figure R1: Comparison of Intensity Scales in Daniell (2014, in his Figure 9), after the work of Gorshkov and Shenkareva (1960), Barosh (1969), Musson et al. (2010) (Note: in this figure, "Liedu-1980/1999" represents the Chinese Seismic Intensity Scale).

(i) **RC1 comment 7:** "The methodology in the transmission of uncertainty from empirical/analytical fragility database to the intensity-PGA relation is provided in Appendix C. This transmission of uncertainty is important and should preferably be integrated into the main text of the paper."

(ii) Response: Thank you for this suggestion. But since the uncertainty of this newly derived intensity-PGA relationship is mentioned only as a number in Section 5.4, to keep the structure of this work clear and also to narrow down the focus, we still consider that it is better to put the uncertainty transmission methodology in the Appendix part for interested readers to have a further check.

References:

Barosh, P. J.: Use of seismic intensity data to predict the effects of earthquakes and underground nuclear explosions in various geologic settings, US Government Printing Office, 1969.

Daniell, J.: Development of socio-economic fragility functions for use in worldwide rapid earthquake loss estimation procedures, Ph.D. Thesis, Karlsruhe Institute of Technology, Karlsruhe, Germany, 2014.

Ding, B., Sun, J., Du, K. and Luo, huan: Study on relationships between seismic intensity and peak ground acceleration, peak ground velocit, Earthquake Engineering and Engineering Dynamics, 37(2), 26–36, http://dx.doi.org/%2010.13197/j.eeev.2017.02.26.dingbr.004, 2017.

Gorshkov, G. P. and Shenkareva, G. A.: On the Correlation of Seismic Scales, U.S. Joint Publications Research Service, New York, United States, https://apps.dtic.mil/docs/citations/ADA362451, 1960.

Ma, Q., Li, S., Li, S. and Tao, D.: On the correlation of ground motion patterns with seismic intensity, Earthquake Engineering and Engineering Dynamics, 34(4), 83–92, doi:10.13197/j.eeev.2014.04.83.maq.011, 2014.

Musson, R. M., Grünthal, G. and Stucchi, M.: The comparison of macroseismic intensity scales, Journal of Seismology, 14(2), 413–428, 2010.

Part 2: Comments from RC2 and our Responses and Changes in the revised manuscript.

(i) **General comments from RC2:** "This is a very interesting paper tying the fragility curves to vulnerability and through this get a better correlation into conversion of Intensities to PGA. The authors reviewed a large number of data published on Chinese earthquakes since 1975 for two main typologies: RC and Masonry: 69 in terms of Chinese Intensity Scale and 18 on PGA. They used fragility curves obtained from experimental (in function of INT) and from numerical developments (in function of PGA) to obtain a conversion between INT vs PGA. To expand the results obtained to other places around the World, and not only to the Chinese construction, in a tentative to propose a world-wide conversion, they compare the results with other proposals in Europe and US (PERPETUATE; SHARE; GEM; etc.). But before I get convinced with the results presented and consequently to accept the paper I need a response to a few important issues."

(ii) Response: Thank you for your interests and this accurate summarization.

(i) **RC2 comment 1:** "Construction in China is very different from other regions. So the comparison with other regions is very difficult to accept."

(ii) Response: This concern is shared by RC1 as well. The comparison with other international projects with similar focus was added to respond to the comments of one reviewer in the previous reviewing process. Actually, it is a painstaking process to conduct such comparison, since the difference in building types across countries and variation in fragility analysis methods pose great difficulty in doing so. Although a lot of efforts have been made, only one (HAZUS Project) similarity for "Masonry_A" building type was found. Such a grand topic deserves an individual and deep-going study in the future, and it is far from enough to attach it as one section of this current work. Therefore, we decide to remove the comparisons in Section 4.2 and delete the related descriptions in the main context and the figures in the Appendix part.

(iii) Changes in the revised manuscript: Section 4.2 and related descriptions in the context are removed. Figure A5, A6, A7 in the Appendix section are also deleted.

(i) **RC2 comment 2:** "Only two Types RC and Masonry (sub-divided into two sub classes) are considered. EMS-98 has many more!"

(ii) Response: Thank you for pointing this out. In the initial fragility data collection work, we actually collected empirical fragility data for more building types, including soil-wood, brick-wood, brick-concrete, RC, industrial frame, stone-wood, chuandou-timber, wood, stone and soil (these data are also available from the online supplement). As explained in Page 6, Line 11-18, since another focus of our work is trying to develop intensity-PGA relationship by using fragility as the bridge, but for analytical fragility data, they are only available for masonry and RC building types. Compared with other building types, masonry and RC are more widely distributed and have relatively more fragility data. That's why only masonry and RC are used. Due to the lack or incompleteness of building seismic resistance information in some reviewed literature and also to ensure data abundancy, it is subjectively decided to divide masonry/RC into two sub-classes.

(i) **RC2 comment 3:** "The final proposal (TableB2) for each Intensity gets an interval 1:2 and no results for I>X. Other studies show similar intervals but with centre value slightly deviated."

(ii) Response: Thank you for your careful check. We further checked the values in Table B2 and they are the same as those in Chinese Seismic Intensity Scale (GB/T 17742-2008, in Chinese). Compared with previous versions (GB/T 17742-1980, GB/T 17742-1999), the current version (GB/T 17742-2008) provides more accurate

description of reference building type used to derive intensity. The average damage index also changes accordingly. But the correspondence relation between intensity and PGA/PGV are the same in all these three officially issued intensity scales.

(i) **RC2 comment 4:** "Errors on establishing the D1 to D4 or D5 are full of uncertainties and so I do not know if bringing the fragilities into place is reducing the error."

(ii) Response: We agree that assigning building damage to different damage states (e.g. from D1 to D4 or D5) is of varying uncertainty. And one way to reduce such uncertainty could be to introduce more damage states/classes. However, one main application of the assignment of building damage into different states/classes is for later-on risk analysis. The increase of damage states will inevitably enhance the difficulty and complexity in applicating them in post-earthquake field investigations. Therefore, trade-off needs to be made and that may be why currently many countries have five damage classes under use.

From the definition of building fragility, which describes the probability to exceed each damage state at various ground shaking levels. The derivation of building fragility curve (as indicated by Eq. (1)-(2)) is dependent on the pre-definition of each damage state indicator. Therefore, we consider that building fragility only loyally inherits the uncertainty from defining different damage states but is not able to reduce such uncertainty.

The advantage of introducing building fragility is that, it provides a practical way to numerically compare fragilities derived from different empirical/analytical methods and fragility curves can also be attached with uncertainties of different damage states.

(i) **RC2 comment 5**: "The Indicator with people and bicycles is very interesting especially for China as there is much traffic with bikes. For other countries unfortunately, the situation is still too far!"

(ii) Response: Exactly. That's further indicates the difficulty in conducting the comparison of Chinese building fragility with other countries.

(i) **RC2 comment 6**: "There should be a Figure representing graphically the results in Table B2."

(ii) Response: Thank you for this good advice. The following figure indicating the correspondence relation between intensity and PGA/PGV (available for intensity V to X) in Table B2 will be added.

(iii) Changes in the revised manuscript: Accepted. The following Figure R2 is added into the Appendix section as the new Fig. A2.

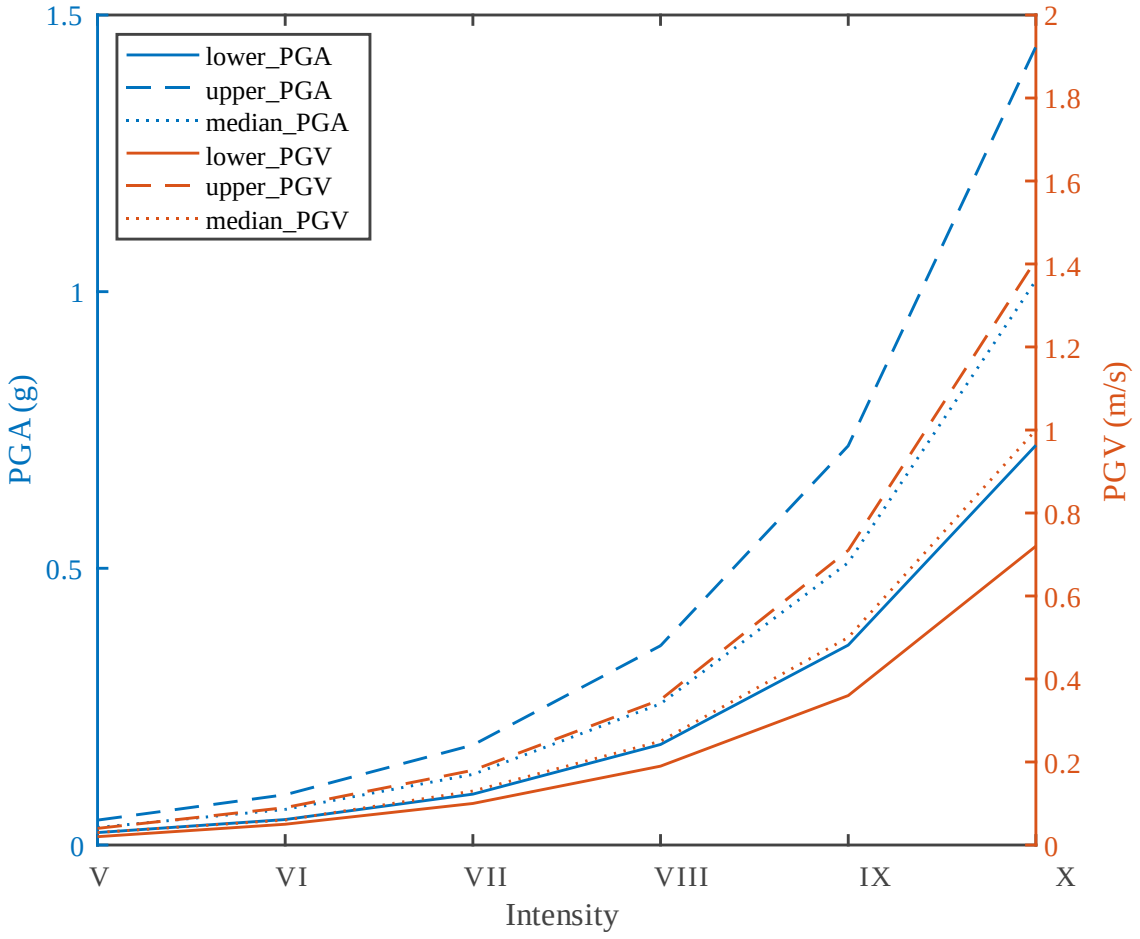

Figure R2: The suggested correspondence relation between intensity and PGA/PGV range by Chinese Official Seismic Intensity Scale (GB/T 17742-2008, as listed in Table B2).

(i) **RC2 comment 7:** "Formula (5) is very old in California".

(ii) Response: We're aware of the current trend that the bilinear function is used to regress the relation between PGA and intensity, based on a rich bunch of observational PGA/PGV and intensity data (e.g. Worden et al., 2012). However, in our work, to develop the relation between intensity and PGA by using fragility as the bridge, the regression relation between ln(PGA) and intensity should be linear, as explained in Page 11 Line 35-Line 8 (Page 12) and derived by Eq. (4).

(i) **RC2 comment 8:** "Fig 3 and 4 should have line to be more understandable."

(ii) Response: For empirical fragility data in Fig. 3, they are digitalized from many post-earthquake surveys and thus are difficult to be represented by one single line.

For analytical fragility data in Fig. 4, they are also digitalized from individual papers or theses for PGA levels like 0.1g, 0.2g, 0.3g…, which are also discrete. Although the original analytical fragility curves are continuous, but not all the literature we scrutinized provided the formula of their fragility curves.

Therefore, all the fragility data in Fig. 3 and 4 are discretely digitalized from different literature, and it is difficult to add lines to these data when putting them together. That's why the following box-plot method will be applied to remove the outliers and find the median fragility for each intensity/PGA level.

(i) **RC2 comment 9:** "Fig 5 and 6 should have line and same color."

(ii) Response: For typical box-plot method, there is actually no line attached. Regretfully, it is also not common to do so. The change of the building fragility with intensity/PGA level can be estimated from the median fragility value (as indicated by the red line and the blue dot within each box of Fig. 5 and Fig. 6, respectively). And the median fragility curve will be represented by lines in Fig. 7 and Fig. 8. But we will adopt your advice to replot Fig. 6.

(iii) Changes in the revised manuscript: Partially accepted. Fig. 6 is updated by the following Figure R3.

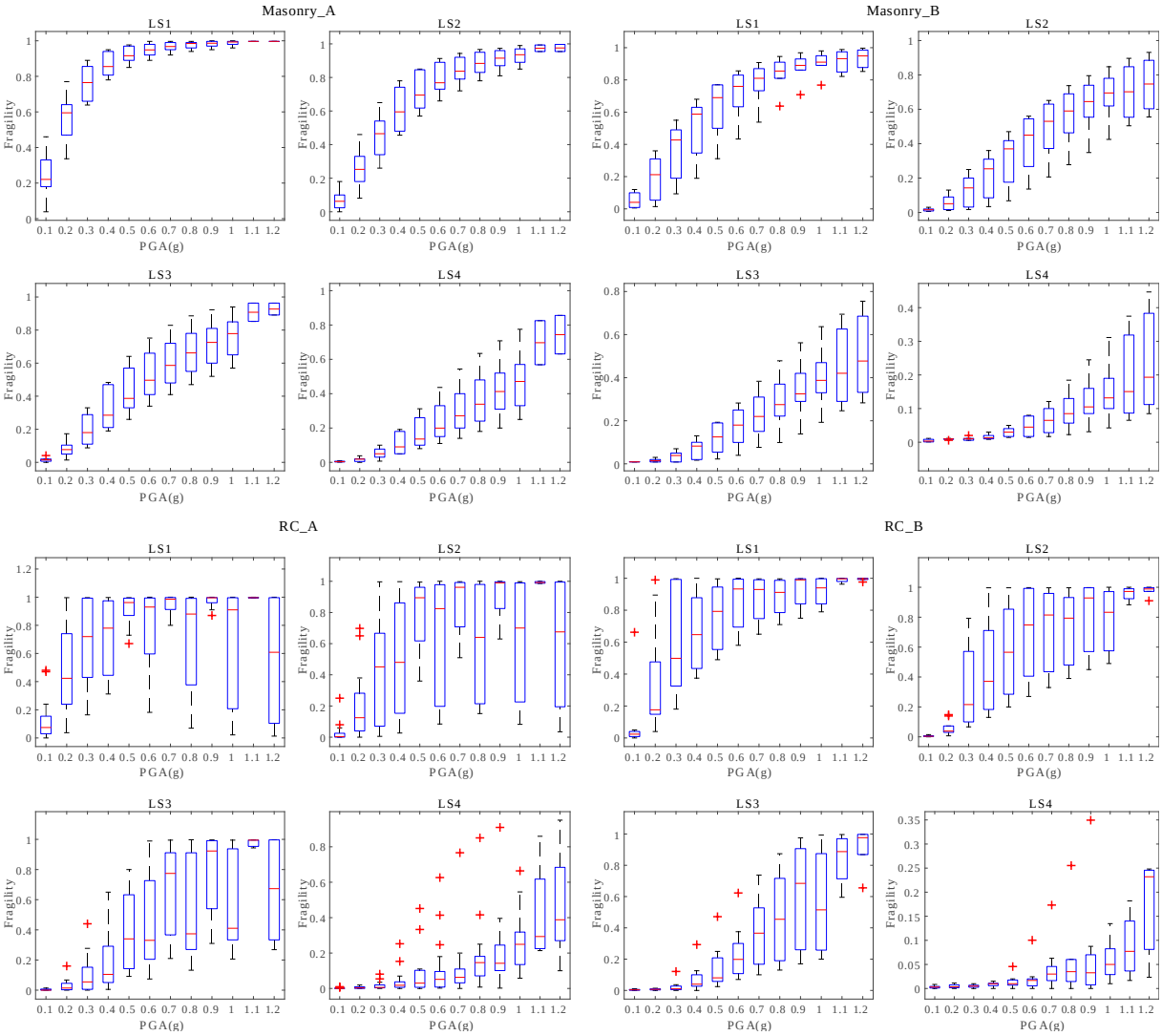

Figure R3: Replotted Figure 6 to keep the same color as Figure 5 in the main context.

(i) **RC2 comment 10:** "Fig A1 could be merged with Fig 7 and Fig A2 with Fig 8."

(ii) Response: Thank you for this good idea. We'll do this.

(iii) Changes in the revised manuscript: Accepted. Fig. 7 and Fig. 8 are updated by the following Fig. R4 and R5, in which the median fragility curve is combined with the error-bar analysis in Appendix Fig. A1 and Fig. A2, respectively. The original Fig. A1 and Fig. A2 are removed.

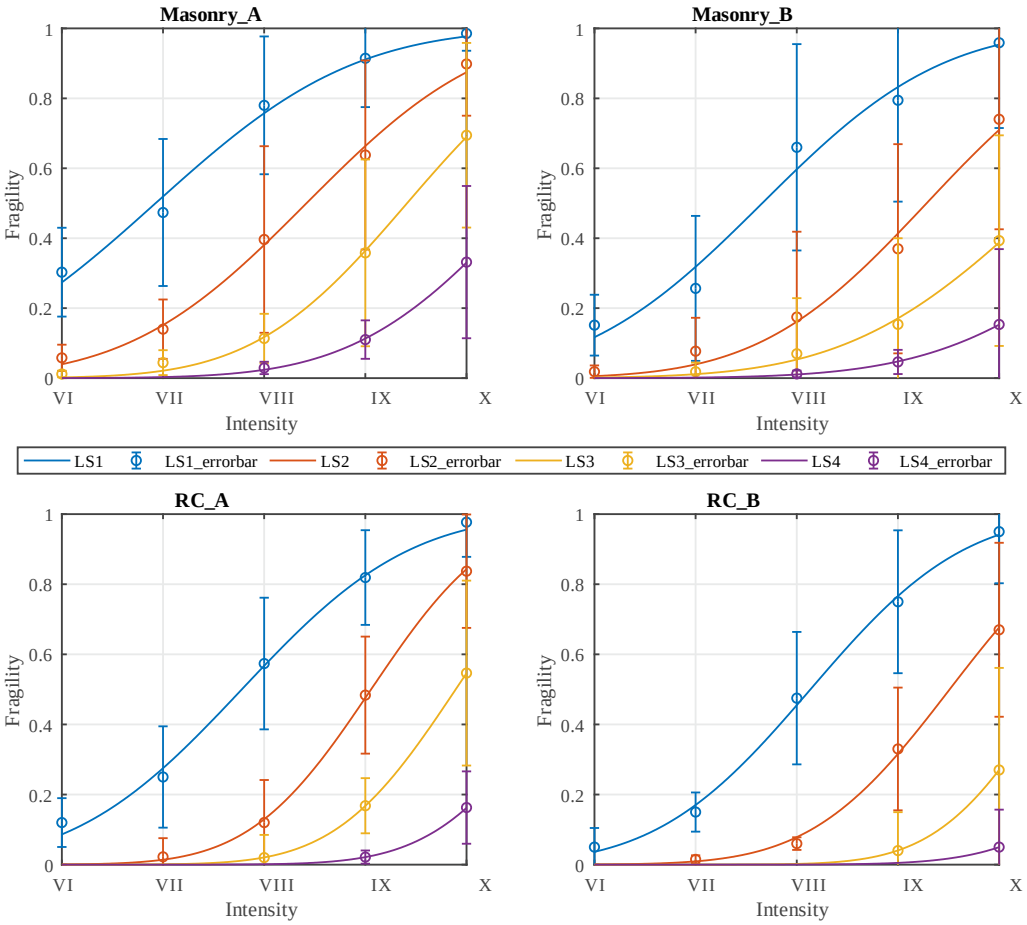

Figure R4: Updated Fig. 7, merged with original Fig. A1 in the Appendix.

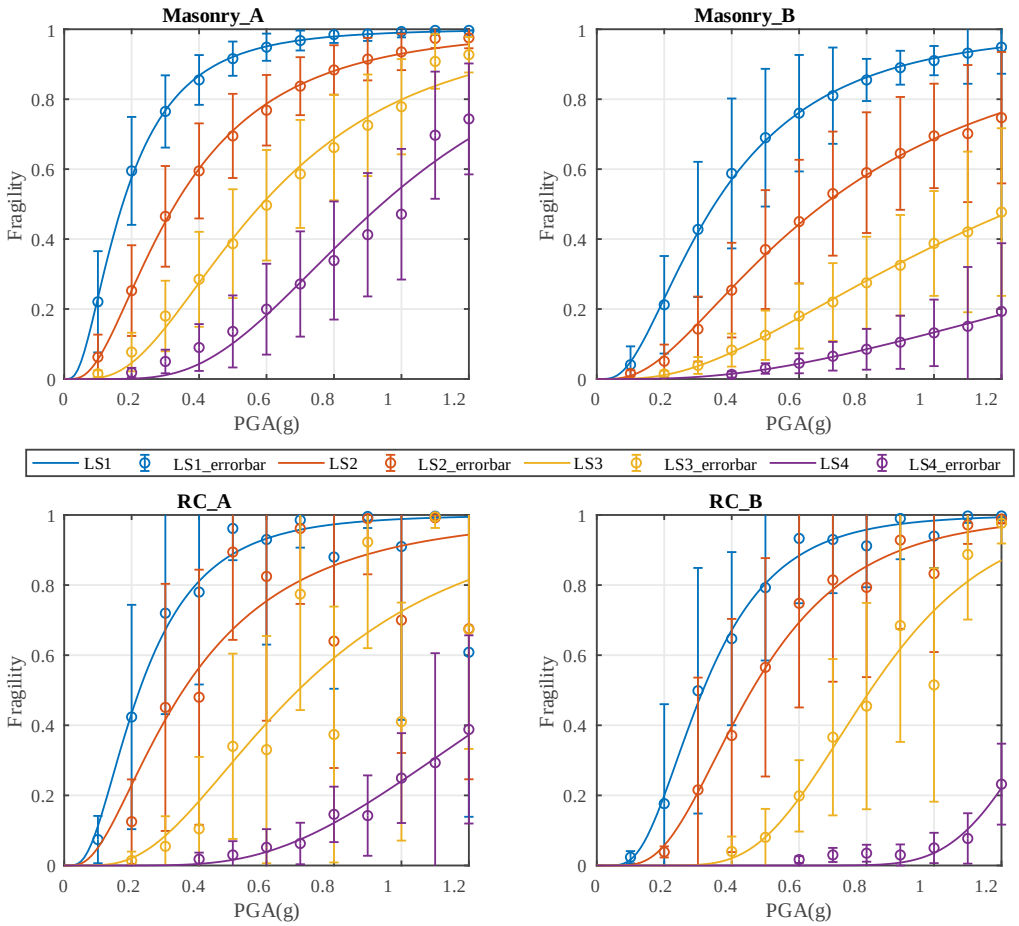

Figure R5: Updated Figure 8, merged with original Fig. A2 in the Appendix.

(i) **RC2 comment 11:** "Figs A6 and A7 are impossible to read!"

(ii) Response: Sorry for this inconvenience. Since the comparison of Chinese building fragility with that in other countries is a quite complex issue and deserves to be studied individually (as explained in above responses), we decide to remove this part from this current manuscript. Thus, Fig. A5, A6, A7 will also be removed.

(iii) Changes in the revised manuscript: Based on the responses to previous comments, Fig. A5-A7 are removed.

(i) **RC2 comment 12:** "Title could be slighted changed, inverting the order of ideas."

(ii) Response: Thank you for this proposal. However, first of all, the review of building fragility has been considered as a challenging task, since different approaches and methodologies are spread across scientific journals, conference proceedings, technical reports and software manuals, hindering the creation of an integrated framework that could allow the visualization, acquisition and comparison between all the existing curves. Therefore, the first focus of our work is to conduct such a review. Secondly, the derivation of intensity-PGA relation by using fragility as the bridge remains to be a tentative approach and uncertainties in between are difficult to fully handle, although we've tried hard to develop the uncertainty transmission methodology in Appendix C. In this regard, we think it is more appropriate to mention this part as an implication from the review of building fragility.

(iii) Changes in the revised manuscript: Given the above consideration, it is more appropriate to keep the title as it is.

(i) **RC2 comment 13:** "I found several inconsistencies in the Reference List Attached Doc (References Corrections)."

(ii) Response: Thank you very much for your careful check!

(iii) Changes in the revised manuscript: Accepted. Such inconsistencies in the revised version are rectified.

Reference:

Worden, C. B., Gerstenberger, M. C., Rhoades, D. A. and Wald, D. J.: Probabilistic Relationships between Ground-Motion Parameters and Modified Mercalli Intensity in California, Bulletin of the Seismological Society of America, 102(1), 204–221, doi:10.1785/0120110156, 2012.

Review of fragility analyses for major building types in China with new implications for intensity-PGA relation development

Danhua Xin[1,2,*], James Edward Daniell[1,2,3], Friedemann Wenzel[1]

[1]Center for Disaster Management and Risk Reduction Technology (CEDIM) and Geophysical Institute, Karlsruhe Institute of Technology, Hertzstrasse 16, 76187, Karlsruhe, Germany

[2]Department of Earth and Space Sciences, Southern University of Science and Technology, 1088 Xueyuan Avenue, Shenzhen 518055, Guangdong Province, China

[2,3]General Sir John Monash Scholar, The General Sir John Monash Foundation, Level 5, 30 Collins Street, Melbourne,Victoria, 3000, Australia

[*]*Correspondence to*: Danhua Xin (danhua.xin@kit.edu)

Formatted: Superscript

Formatted: Superscript

Abstract. The evaluation of the seismic fragility of buildings is one key task of earthquake safety and loss assessment. Many research reports and papers have been published over the past four decades that deal with the vulnerability of buildings to ground motion caused by earthquakes in China. We first scrutinized 69 papers and theses studying building damage for earthquakes occurred in densely populated areas. They represent observations where macro-seismic intensities have been determined according to the Chinese Official Seismic Intensity Scale. From these many studies we derived the median fragility functions (dependent on intensity) for four damage limit states of two most widely distributed building types: masonry and reinforced concrete. We also inspected 18 publications that provide analytical fragility functions (dependent on PGA) for the same damage classes and building categories. Thus, a solid fragility database based on both intensity and PGA is established for seismic prone areas in mainland China. A comprehensive view of the problems posed by the evaluation of fragility for different building types is given. ~~Necessary comparison with international projects with similar focus is conducted.~~ Based on the newly collected fragility database, we propose a new approach in deriving intensity-PGA relation by using fragility as the bridge and reasonable intensity-PGA relations are developed. This novel approach may shed light on new thought in decreasing the scatter in traditional intensity-PGA relation development, i.e., by further classifying observed macro-seismic intensities and instrumental ground motions based on difference in building seismic resistance capability.

1 Introduction

Field surveys after major disastrous earthquakes have shown that poor performance of buildings in earthquake affected areas is the leading cause of human fatalities and economic losses (Yuan, 2008). The evaluation of seismic fragility for existing building stocks has become a crucial issue due to the frequent occurrence of earthquakes in the last decades (Rota et al., 2010). Building fragility curves, defined as expected probability of exceeding specific building damage state under given earthquake ground shaking, have been developed for different typologies of buildings. They are required for the estimation of fatalities and monetary losses due to building structural damage. The development of fragility curves can be divided mainly into two approaches: empirical methods and analytical methods. Empirical methods are based on post-earthquake surveys for groups

of buildings and considered to be the most reliable source, because they are directly correlated to the actual seismic behaviour of buildings (Maio and Tsionis, 2015). Numerous post-earthquake investigations have been conducted for groups of buildings to derive the empirical damage matrices. A damage matrix is a table of predefined damage states and percentages of specific building types at which each damage state is exceeded due to particular macro-seismic intensity levels. However, as pointed out by Billah and Alam (2015), empirical investigations are usually limited to particular sites or seismo-tectonic/geotechnical conditions with abundant seismic hazard and lack generality. Moreover, they usually refer to the macro-seismic intensity, which is not an instrumental measure but is based on a subjective evaluation (Maio and Tsionis, 2015). By contrast, analytical methods are based on static and dynamic nonlinear analyses of modelled buildings, which can produce slightly more detailed and relatively more transparent assessment algorithms with direct physical meaning (Calvi et al., 2006). Therefore, analytical methods are conceived to be more reliable than empirical results (Hariri-Ardebili and Saouma, 2016). Nevertheless, variations in the different practices of analytical fragility studies, such as selection of seismic demand inputs, use of analysis techniques, characterisation of modelling structures, definition of damage states thresholds as well as usage of damage indicators by different authorities, can create discrepancies among various analytical results even for exactly the same building typology. In addition, analytical fragility studies for groups of buildings are computationally demanding and often technically difficult to perform.

Despite the limitations of each fragility analysis method, both empirical and analytical fragility curves are essential in conducting seismic risk assessment. However, the application of the existing fragility curves has been considered as a challenging task, since different approaches and methodologies are spread across scientific journals, conference proceedings, technical reports and software manuals, hindering the creation of an integrated framework that could allow the visualization, acquisition and comparison between all the existing curves (Maio and Tsionis, 2015). In this regard, the first purpose of this study is to describe and examine available fragility curves, specially developed for Chinese buildings from 87 papers and theses using empirical and analytical methods. The median fragility functions from these previous research findings for the main building types in seismic prone areas in mainland China are then outlined ~~and compared with international projects with similar focus~~.

Furthermore, based on the empirical and analytical fragility database collected, the second purpose of this work is to propose a new approach in deriving intensity-PGA relation by using fragility as the bridge. The main concern behind this attempt is that intensity-PGA relation is quite essential in seismic hazard assessment, while traditional practices in deriving such a relation are generally region-dependent and have large scatter (Caprio et al., 2015). Traditionally, intensity-PGA relations are developed using instrumental PGA records and empirical intensity observations within the same geographical range. In this work, we try to establish intensity-PGA relation using fragility as conversion media. Formally, this is achieved by the elimination of the fragility values from the fragility–intensity and from the fragility–PGA relation. Theoretically, reasonable results should emerge if the building types used in analytic fragility analyses and those investigated in the empirical field surveys are close enough.

This study is organized as follows. In Section 1, the necessity of fragility database construction and the pros and cons of main fragility analysis methods are briefly introduced. In Section 2, a literature review of fragility studies in mainland China and related concepts is provided. Section 3 presents the discrete fragility database extracted

from reviewed papers and theses. In Section 4, median empirical and analytical fragility curves and their scatter are derived for major building types in seismic prone areas in mainland China. ~~Comparisons with international projects with similar focuses are also conducted in this section.~~ In Section 5, we introduce in detail our new approach in developing intensity-PGA relation by using fragility as bridge, which is quite comparable with relation developed by traditional practice. In Appendix and Code/Data availability, accesses to supplementary documents mentioned in the context are provided.

2 Review of building fragility studies in mainland China

2.1 Empirical method

As documented in Calvi et al. (2006), the first application of empirical method to investigate building fragility at large geographical scale was carried out in the early 1970s. In mainland China, since the 1975 Haicheng M7.5 earthquake, around 112 post-earthquake surveys have been conducted for M≥4.7 earthquakes (Ding, 2016). Currently, the main processes in post-earthquake field investigation and macro-seismic intensity determination in mainland China basically follow the workflow proposed by Hu (1988) based on the field work of Tonghai earthquake in the 1970s (Wang et al., 2007). In this workflow, the key concept of "average damage index" is introduced. That means, in each post-earthquake field survey unit (village/town/street), the number of different types of buildings in each damage state are firstly investigated; median damage index of five damage states D5, D4, D3, D2, D1 as defined in ~~GB17742~~ GB/T 17742-2008 are used in later on calculation, namely 0.93, 0.70, 0.43, 0.20, 0.05 for these five damage states respectively. For each building type in each field survey unit, the corresponding average damage index is derived by summarizing the products of percentage of building in each damage state and its damage index. Generally, there should be one or two predefined reference building types, thus the average damage index of other surveyed building types can be further scaled to the damage index of the reference building type. In the end, the overall average damage index for each survey unit is calculated by summarizing the products of each building type's scaled damage index and that building type's weight in the survey unit. Once the average damage index in the survey unit is determined, the corresponding macro-seismic intensity can be directly derived from the predefined empirical relation between macro-seismic intensity and damage index of reference building type (~~GB17742~~ GB/T 17742-2008). In mainland China, currently three reference building types are used to determine macro-seismic intensity: (1) Type A: wood-structure, soil/stone/brick-made old building; (2) Type B: single- or multi-storey brick masonry without seismic resistance; (3) Type C: single- or multi-storey brick masonry sustaining shaking of intensity degree VII. A detailed building structural damage state description for judgement of macro-seismic intensity scale in China is given in Table B2 (a non-official translation of the latest version of ~~China~~ Chinese ~~seismic~~ Seismic ~~intensity~~ Intensity ~~scale~~Scale: ~~GB17742~~ GB/T 17742-2008; modified after CSIS, 2019). Comparison of the Chinese seismic intensity scale with other internationally adopted scales was conducted by Daniell (2014) and their relationship is shown in Fig. A1. The correspondence relations between intensity-PGA and intensity-PGV in GB/T 17742-2008 are also graphically illustrated in Fig. A2 in the Appendix section.

Given the importance of building fragility in seismic risk assessment and loss mitigation, in total we reviewed 87 existing fragility analyses from papers and theses for the main building typologies in seismic prone areas in mainland China. It's worth to note that, in Ding (2016), a very detailed collection of empirical fragility database was provided for 112 M≥4.7 events since the 1975 M7.5 Haicheng earthquake based on available post-

earthquake surveys. However, due to the lack of building seismic resistance capability information in this database, it is not suitable for our later-on fragility analysis. Thus, we did not use this database and instead collected our own empirical fragility database from individual publications and M.S./Ph.D theses. In mainland China, the main building types of concern are masonry and reinforced concrete (RC) buildings (Sun and Chen, 2009), given the wide distribution of masonry in rural and township areas and the increasing popularity of RC buildings in urban areas. Historic earthquakes that caused serious building damage mainly occurred in seismic prone provinces including **Sichuan** (Chen et al., 2017; Gao et al., 2010; He et al., 2002; Li et al., 2015; Li et al., 2013; Sun et al., 2013; Sun et al., 2014; Sun and Zhang, 2012; Ye et al., 2017; Yuan, 2008; Zhang et al., 2016), **Yunnan** (He et al., 2016; Ming et al., 2017; Piao, 2013; Shi et al., 2007; Wang et al., 2005; Yang et al., 2017; Zhou et al., 2007; Zhou et al., 2011), **Xinjiang** (Chang et al., 2012; Ge et al., 2014; Li et al., 2013; Meng et al., 2014; Song et al., 2001; Wen et al., 2017), **Qinghai** (Piao, 2013; Qiu and Gao, 2015), **Fujian** (Bie et al., 2010; Zhang et al., 2011; Zhou and Wang, 2015) and **other seismic active zones** (A, 2013; Chen, 2008; Chen et al., 1999; Cui and Zhai, 2010; Gan, 2009; Guo et al., 2011; Han et al., 2017; He and Kang, 1999; He and Fu, 2009; He et al., 2017; Hu et al., 2007; Li, 2014; Liu, 1986; Lv et al., 2017; Ma and Chang, 1999; Meng et al., 2012; Meng et al., 2013; Shi et al., 2013; Sun and Chen, 2009; Sun, 2016; Wang et al., 2011; Wang, 2007; Wei et al., 2008; Wu, 2015; Xia, 2009; Yang, 2014; Yin et al., 1990; Yin, 1996; Zhang and Sun, 2010; Zhang et al., 2017; Zhang et al., 2014; Zhou et al., 2013). The main outputs of these post-earthquake surveys are empirical damage probability matrices (DPMs), which can be used to derive the discrete conditional probability of exceeding predefined damage limit states under different macro-seismic intensity degrees. That is, for the DPMs, macro-seismic intensity degree is usually used as the ground motion indicator. ~~In mainland China, detailed definition of each intensity degree is provided in Chinese Official Seismic Intensity Scale GB17742~~ GB/T 17742~~-2008 (see the non-official English translation in Appendix Table B2).~~

2.2 Analytical method

As summarized in Introduction section, the main drawback of empirical method lies in the subjectivity on allocating each building to a damage state and the lack of accuracy in the determination of the macro-seismic intensity affecting the region (Maio and Tsionis, 2015). Furthermore, the interdependency between macro-seismic intensity and damage as well as the limited or heterogeneous empirical data are commonly identified as the main difficulties to overcome in the calibration process of empirical approaches (Del Gaudio et al., 2015). By contrast, analytical methodologies produce more detailed and transparent algorithms with direct physical meaning, that not only allow detailed sensitivity studies to be undertaken, but also allow for the straightforward calibration of the various characteristics of the building stock and seismic hazard (Calvi et al., 2006). Different from the empirical fragility that is directly collected from post-earthquake survey, the derivation of analytical fragility curve is often based on nonlinear fine-element analysis. Popular analytical methods include push-over analysis (Freeman, 1998; Freeman, 2004), adaptive push-over method (Antoniou and Pinho, 2004), and incremental dynamic analysis (IDA) (Vamvatsikos and Cornell, 2002; Vamvatsikos and Fragiadakis, 2010). Within these approaches, most of the methodologies available in literature lie on two main and distinct procedures: the correlation between acceleration or displacement capacity curves and spectral response curves, as the well-known HAZUS or N2 methods (FEMA, 2003; Fajfar, 2000), and the correlation between capacity curves and acceleration time histories, as proposed in Rossetto and Elnashai (2003).

The major steps in using analytical methods to study building fragility include: the selection of seismic demand inputs, the construction of building models, the selection of damage indicator and the determination of damage limit state criteria (Dumova-Jovanoska, 2000). To combine empirical post-earthquake damage statistics from actual building groups with simulated/analytical damage statistics from modelled building types under consideration, we examined quite a few studies deriving analytical fragility curves for masonry and RC buildings in mainland China. The analysis techniques in these studies vary from static push-over analysis or adaptive push-over method (Cui and Zhai, 2010; Liu, 2017), to dynamic history analysis or incremental dynamic analysis (Liu et al., 2010; Liu, 2014; Liu, 2014; Sun, 2016; Wang, 2013; Yang, 2015; Yu et al., 2017; Zeng, 2012; Zheng et al., 2015; Zhu, 2010) as well as based on necessary statistical assumptions (Fang, 2011; Gan, 2009; Guo et al., 2011; Hu et al., 2010; Zhang and Sun, 2010).

2.3 Damage state definition

As predefined, building fragility describes the exceedance probability of specific damage state given an ensemble of earthquake ground motion levels. To describe the susceptibility of building structure to certain ground motion level, four damage limit states are used to discriminate between different strengths of ground shaking: slight damage (LS1), moderate damage (LS2), serious damage (LS3) and collapse (LS4). These four limit states divide the building into five structural damage states, namely negligible (D1), slight damage (D2), moderate damage (D3), serious damage (D4) and collapse (D5). The relation between limit states and structural damage states is illustrated by Fig. 1. Hereafter, fragility curves in this study specifically refer to the probability of exceeding four damage limit states (LS1, LS2, LS3, LS4) under different ground motion levels.

Standard definitions of building structural damage states have been issued in different countries and areas. In the European Macro-seismic Scale 1998 (EMS1998) proposed by European Seismological Commission (ESC), five grades of structural damage are defined: negligible to slight damage (Grade 1), moderate damage (Grade 2), substantial to heavy damage (Grade 3), very heavy damage (Grade 4) and destruction (Grade 5). In the HAZUS99 Earthquake Model Technical Manual, developed by Department of Homeland Security, Federal Emergency Management Agency of the United States (FEMA) in 1999, generally four structural damage classes are used for all building types: slight damage, moderate damage, extensive damage and complete damage. Other damage state classifications like MSK1969 proposed by Medvedev and Sponheuer (1969) and AIJ1995 (Nakamura, 1995) in Japan issued by Architectural Institute of Japan are summarized in Table 1. In mainland China, the latest standard ~~GB17742~~ GB/T 17742-2008 was issued in 2008 by China Earthquake Administration (CEA), in which detailed damage to structural and non-structural components are defined for each damage state (Table 2).

In empirical method, fragility curve is derived from damage probability matrices (DPMs) based on post-earthquake field surveys. DPMs give the proportions of buildings in each structural damage state (D1, D2, D3, D4, D5), and they can be used to derive the probability of exceeding each damage limit state $P[LS_i]$ (i=1,2,3,4), as illustrated in Eq. (1):

$$P[LS_i] = 1 - P[D_i]\ (i = 1); \quad P[LS_i] = P[LS_{i-1}] - P[D_i]\ (i = 2 \dots N) \tag{1}$$

where N refers to the total number of damage limit states (here N=4); for each building type, $P[D_i]$ refers to the proportion of building in each structural damage state i.

In analytical method, fragility curve is derived by Eq. (2), with the assumption that building response to seismic demand inputs follows the lognormal distribution:

$$P[LS|S_d] = \Phi\left[\frac{1}{\beta_{LS}}\ln\left(\frac{S_d}{S_{C|LS}}\right)\right] \quad (2)$$

where $P[LS|S_d]$ is the probability of being in or exceeding damage limit state LS due to ground motion indicator S_d (e.g. the inter-storey displacement, the spectral acceleration, the peak ground acceleration etc.); $S_{C|LS}$ refers to the median value of damage state indicator at which the building reaches the threshold of the damage state LS; β_{LS} represents integrated uncertainties from seismic demand input, building capacity and model uncertainty, generally within the range of 0.6-0.8; $\Phi[\ ]$ is the normal cumulative probability distribution.

3 Fragility database analysis

3.1 Building typology and seismic resistance level classification

During the past four decades, more than 2000 M≥4.7 earthquakes have occurred in mainland China and its neighbouring areas (Xu et al., 2014). Up to 2014, post-earthquake field surveys have been conducted for at least 112 damaging earthquakes that occurred in the densely populated areas in mainland China, since the 1975 M7.3 Haicheng earthquake (Ding, 2016). These damaging earthquakes mainly clustered in seismic prone provinces in southwestern China (e.g. Sichuan, Yunnan) and western China (e.g. Xinjiang Uygur, Tibet, Qinghai), as shown in Fig. 2. The main building types in these areas are featured by masonry, reinforced concrete (RC), brick-wood, soil, stone as well as chuandou-timber (a typical building type in mountainous area of Tibet, Qinghai and Sichuan). Due to the limitation in fragility data abundance, we mainly focus on studying the seismic fragility of the two most widely distributed building types: masonry and RC buildings (Sun and Chen, 2009). Masonry buildings are mainly composed of brick and concrete. RC buildings include building structures such as RC core wall, frame structure and frame-shear wall.

The seismic resistance level of masonry and RC buildings is further divided into two classes: level A and level B. The assignment of seismic resistance level in this study is mainly based on supplementary information given in each scrutinized literature, including building age, construction material, seismic resistance code at construction time, load-bearing structure etc. Given the changes in building quality and corresponding code standard over the past four decades in China, buildings constructed in different ages though with the same nominal resistance level of each period, are reassigned with different seismic resistance levels according to the latest standard. The referred grouping criteria is given in Table 3 (*more building classification details can be found from the online supplement*). Generally, "level A" includes buildings with seismic resistance level assigned as pre/low/moderate-code, and "level B" includes buildings assigned as high-code.

3.2 Outlier check

After grouping the empirical and analytical fragilities based on building type (masonry and RC) and seismic resistance level (A and B) in Sect. 3.1, the empirical fragility database based on macro-seismic intensity (Fig. 3)

and analytical fragility database based on PGA (Fig. 4) for four damage limit states (LS1, LS2, LS3, LS4) are thus constructed (*data can be found from the online supplement*). The Y-axis "fragility" of Fig. 3 and Fig. 4 refer to the exceedance probability of each damage limit state at each ground motion level. As can be seen, the scatter of fragilities varies across building types and seismic resistance levels. For empirical fragilities, the scatter may relate to the uneven abundance of damage data for buildings investigated in post-earthquake field surveys, the subjective judgement of damage states as well as the rough division of building structure types. For analytical fragilities, the scatter may come from the difference in the selection of seismic demand inputs, the use of analysis techniques, the detailing of the modelled building structure, the definition of damage state as well as the difference in damage indicators used by different researchers. Thus, before deriving consecutive building fragility curves from these discrete fragility data in Fig. 3 and Fig, 4, the outliers need to be firstly removed from these originally collected datasets.

To figure out the outliers in the originally collected fragility database, the box-plot check method was applied. For each building type (Masonry_A, Masonry_B, RC_A, RC_B) and in each damage limit state (LS1, LS2, LS3, LS4), the corresponding series of fragility data was sorted from the lowest to the highest value. Three quantiles (Q_1, Q_2, Q_3) were used to divide each fragility series into four equal-sized groups and they correspond to the 25%, 50% and 75% quantile value in each series. A discrete fragility value (Q_i) was assigned as an outlier if $Q_i - Q_3 > 1.5 \times (Q_3 - Q_2)$ or $Q_1 - Q_i > 1.5 \times (Q_2 - Q_1)$. The box-plot check results are shown in Fig. 5 for empirical fragility data and in Fig. 6 for analytical fragility data.

4 Derivation of representative fragility curves

After removing outliers, details of the remaining fragility dataset (e.g., the number of data points, median and standard deviation of these data) for each damage state of each building type are ~~plotted in Appendix Fig. A1-A4 and~~ summarized in Appendix Table B1. The change of standard deviation of each fragility series is shown in Fig. A3 and Fig. A4 for empirical and analytical data, respectively. It is worth to iterate that, as aforementioned in the Introduction section, the organization of this study is centred on two focuses. The first one is to construct a comprehensive fragility database for Chinese buildings from 87 papers and theses using empirical and analytical methods, which is one key component of seismic risk assessment. Based on the empirical and analytical fragility database collected, the second focus is to propose a new approach in deriving intensity-PGA relation by using fragility as the bridge. In this regard, a representative fragility curve should be firstly derived for each damage state of each building type, and we refer to use the median fragility values to derive such a curve.

~~4.1 Median fragility curve~~

To derive ~~a~~ the representative fragility curve for each damage limit state (LS1, LS2, LS3, LS4) of each building type (Masonry_A, Masonry_B, RC_A, RC_B) for further study (to derive intensity-PGA relation in Sect. 5), the median values (50% quantile) of each fragility series in Fig. 5 and Fig. 6 are used. For consecutive median fragility curve derivation, cumulative normal distribution is assumed to fit the discrete median empirical fragilities and log-normal distributions is assumed to fit the discrete median analytical fragilities. For each damage limit state of each building type, the parameters μ_{LS} and σ_{LS} in the consecutive fragility curve can be regressed following Eq. (3):

$$P(X|LS) = \Phi\left[\frac{X_{int}-\mu_{LS}}{\sigma_{LS}}\right] \quad or \; P(X|LS) = \Phi\left[\frac{1}{\sigma_{LS}}\ln\left(\frac{X_{PGA}}{\mu_{LS}}\right)\right] \tag{3}$$

where $P(X|LS)$ represents the exceedance probability of each damage limit state LS given ground motion level X (X refers to X_{int}, namely macro-seismic intensity in terms of empirical fragility; and X refers to X_{PGA}, namely PGA in terms of analytical fragility).

The median fragility curves derived from the discrete fragilities for empirical data and for analytical data are plotted in Fig. 7 and Fig. 8, respectively. To better illustrate the scatter of the originally collected discrete fragility data, the error-analysis is attached with each regressed median fragility curve. As can be clearly seen from the regressed fragility curves in Fig. 7 and Fig. 8, there are two obvious trends: (1) for the same building type (masonry or RC), the higher the seismic resistance level (A<B), the lower the building fragility, which applies for all damage limit states; (2) for the same seismic resistance level, RC building has lower fragility than masonry building, which also applies for all damage limit states. These two trends indicate the reliability of the newly collected fragility database, the reasonability of the criteria in grouping building types and seismic resistance levels, as well as the suitability of using median fragility values to develop representative fragility curves for further analysis. However, some extra abnormality is also noteworthy, e.g. in the median fragility curve developed for LS4 of "RC_B" in Fig. 8, the probability to exceed LS4 damage limit state remains 0 even when PGA is higher than 0.8 g, which is obviously not the case in reality. Detailed source of such abnormality and its effect on the intensity-PGA relation to develop will be discussed in Sect. 5.3.

Mathematically, the goodness of fit of the consecutive median fragility curve from discrete median fragilities can be measured by statistical indicator R^2 (Draper and Smith, 2014). Higher R^2 value indicates a better fit of the regressed fragility curve, since it is defined as the ratio between *SSR* and *SST: SSR* is the ***s**um of **s**quares of the **r**egression* ($SSR = \sum_{i=1}^{n}(\hat{y}_i - \bar{y}_i)^2$), and SST is the ***t**otal **s**um of **s**quares* ($SST = \sum_{i=1}^{n}(y_i - \bar{y}_i)^2$); y_i refers to the original discrete fragilities for each damage limit state, $\bar{y}_i$ refers to the mean fragility, $\hat{y}_i$ refers to the predicted fragility by the fitted fragility curve. As shown in Table 4, the R^2 values are generally above 0.95, which indicates the normal or lognormal distribution assumption in Eq. (3) is very suitable to match the discrete fragility datasets. Noticeably, there are also three low R^2 values (≤0.8) in Table 4 for damage limit state LS1, LS2, LS3 of building type "RC_A", which may indicate the low quality (e.g. high scatter) of the originally collected fragility data. As can be cross validated from Fig. 4 and even better Fig. 6 and Fig. 8, the analytical fragility data for "RC_A" are more scattered than for other building types. This thus directly leads to the low R^2 values in fitting the median fragility curve for damage limit state LS1, LS2, LS3 of "RC_A".

~~**4.2 Fragility curve comparison with international projects**~~

~~Given the import role of fragility curve for future seismic risk assessment and loss estimation especially in seismic prone areas, we construct the empirical and analytical fragility database from 87 individual papers and theses. The median and standard deviation of the fragility series for each damage state of each building type are plotted in Appendix Fig. A1-A4 and listed in Appendix Table B1. To derive new intensity-PGA relation by using fragility as the bridge, the median fragility curves for masonry and RC building types with seismic resistance levels A and B are regressed, as shown in Fig. 7 and Fig. 8. While, the robustness of these median fragility curves varies across damage states and building types, as will be discussed in detail in Sect. 5.3. Here, to~~

better place such a review work, it is worth to compare it with international projects with similar focus. Therefore, we also checked the fragility outputs from several international projects, including PERPETUATE, SYNER-G, PAGER, HAZUS and GEM. Based on the detailed analysis in Sect. 5.3, median fragility curves developed for building type "Masonry_A" are of relatively highest robustness. Thus, the comparison of our median fragility curves with these international projects (in terms of PGA) will be based on "Masonry_A" building type only. To avoid over complexity, the scatter attached to each fragility curve is not taken into account in this comparison.

4.2.1 PERPETUATE project

The main goal of European PERPETUATE project was to develop European guidelines for evaluation and mitigation of seismic risk to cultural heritage assets, applicable in the European and other Mediterranean countries. As written in their project homepage, the risk assessment of heritage buildings requires the assessment of both architectonic and artistic assets contained in them, which needs improvement in methods of analysis and assessment procedures rather than in intervention techniques for common buildings and infrastructures. Besides that, a verification approach in terms of displacement rather than in terms of strength is more reliable and effective for heritage building. However, the fragilities collected in this study are mainly for general masonry and RC buildings and mainly in terms of macro-seismic intensity or PGA, not displacement. Therefore, the fragility outputs from PERPETUATE project and our study are not so comparable.

4.2.2 SYNER-G project

European SYNER-G project focused on reviewing fragility for masonry and RC buildings in Europe, including the collection of existing fragility functions, building recategorization, and harmonization of intensity measure and limit states. In the final output of SYNER-G project, fragility curves were given in terms of PGA, with some of them converted from macro-seismic intensity or spectral acceleration (SA) (Crowley et al., 2011a; Crowley et al., 2011b; Kaynia et al., 2013; Pitilakis et al., 2014). Comparisons between mean fragility curves developed in SYNER-G project (Crowley et al., 2011b; refer to Table 6.3 and Table 6.5) with our median analytical fragility curves for "Masonry_A" building type are plotted in Fig. A5. It is noteworthy that, in SYNER-G outputs, the typically four damage limit states were further harmonized into two: yielding damage state (LS2) and collapse state (LS4).

As can be seen from Fig. A5, the fragility in SYNER-G project for typical European masonry buildings is much higher than "Masonry_A" in this study. The discrepancy of fragility for masonry between SYNER-G (Silva et al., 2014) and this study is potentially related to the following factors. Firstly, the difference in use of ground motion indicator (part of SYNER-G's PGA-related fragility curves are converted from intensity, SA related fragility curves; our analytical fragility curves are purely PGA-related) may play a role. Besides that, difference in building classification is difficult to accurately calibrate but certainly contributes to the final fragility discrepancy. Furthermore, the harmonization of damage limit states in SYNER-G project (from four to two) makes the fragility difference between these two damage states subtle as shown in Fig. A5, and also hinders the fragility comparison for each damage limit state accordingly. Lastly, in SYNER-G project, the mean fragility curves are provided; but in this study, median fragility curves are developed for nominally similar masonry

buildings. In all, these differences combined together lead to the fragility discrepancy for general masonry buildings in our fragility curves and those in SYNER-G project.

4.2.3 PAGER project

The ongoing PAGER project (Prompt Assessment of Global Earthquakes for Response) of United States is an automated system specialized in estimating the seismic ground shaking distribution, the number of people and settlements exposed to that severe shaking, and the scale/range of possible fatalities and economic losses. For these purposes, vulnerability functions are used, which are different from the fragility functions we focus on in this study. The main difference lies in that, vulnerability functions can be derived either directly from historic damage information, or indirectly from fragility function combined with consequence functions, which describe the probability of loss given a level of performance (e.g. collapse damage state). Thus, direct comparison between the outputs of PAGER project and our study is not available.

4.2.4 HAZUS project

The ongoing HAZUS project of United States, is developed and updated to provide local, state and regional officials with the tools necessary to plan and stimulate efforts to reduce risk from earthquakes and to prepare for emergency response and recovery from an earthquake (FEMA, 2003; FEMA, 2008). HAZUS offers a series of fragility curves for typical building types based on HAZUS building taxonomy. Here for comparison with our fragility curves for "Masonry_A", we extracted HAZUS fragility curves developed for two specific masonry building types: mid-rise reinforced masonry bearing walls with wood or metal deck diaphragms (RM1M) and high-rise reinforced masonry bearing walls with precast concrete diaphragms (RM2H) from HAZUS Earthquake Technical Manual (refer to Table 5.16a-d). These fragility curves are based on median spectral displacement of the damage state of interest and an assumed demand spectrum shape that relates spectral response to PGA. The reference spectrum used to derive HAZUS fragility curve represents ground shaking of a large magnitude (i.e. M ≈7.0) western United States earthquake for soil sites (e.g. site class D) at site to source distances of 15km or greater.

Comparisons between the fragility curves of HAZUS for "RM1M, RM2H" and those developed in this study for "Masonry_A" are plotted in Fig. A6 (RM1M) and Fig. A7 (RM2H). In HAZUS four code levels (pre/low/moderate/high) are provided; but in this study, only two seismic resistance levels "A" and "B" are assigned to the analytical fragilities extracted from individual literature (*more details can be found from online supplement*). As can be seen from Fig. A6 and Fig. A7, the median fragility of our "Masonry_A" is basically between the median fragility of high-code and moderate-code of "RM1M" and "RM2H" building types, which indicates the compatibility between HAZAU and our median fragility curves for general masonry buildings, compared with the mean fragility curves in SYNER-G project.

4.2.5 GEM project

The ongoing Global Earthquake Modelling (GEM) project, is motivated to "serve the public good in a collaborative, credible, open and transparent manner, and to make risk assessment inclusive to create a holistic culture of awareness and resilience, bringing a once-scarce resource available to all sectors and beneficiaries".

~~GEM project has integrated outputs from three other European projects: SHARE, SYNER-G and NERA. SHARE focuses on seismic hazard harmonization in Europe and covers all of Europe and the Maghreb countries. The hazard model is developed with the OpenQuake Engine. SYNER-G partners developed a unified methodology and tools for systemic vulnerability assessment in Europe. NERA focused on the creation of a European research infrastructure for risk assessment and mitigation. Besides the fragility outputs from SYNER-G project, GEM online fragility database also integrates fragility curves from HAZUS (Yepes-Estrada et al., 2016). Therefore, we do not repeat the comparison with GEM fragility curves developed for European and American building types. For mainland China, the fragility curves integrated in GEM database is solely from Tang et al. (2011) developed for Chinese schools, and only for RC building with spectral acceleration (SA) as the ground motion indicator. To avoid uncertainty introduced from converting SA to PGA, here we also skip the comparison with fragility curves in Tang et al. (2011).~~

5 New approach in deriving intensity-PGA relation

Intensity-PGA relation has an important application in seismic hazard assessment, since the use of macro-seismic data can compensate for the lack of ground motion records and thus help in reconstructing the shaking distribution for historical events. Traditionally, intensity-PGA relations are developed using instrumental PGA records and macro-seismic intensity observations within the same geographical range (Bilal and Askan, 2014; Caprio et al., 2015; Ding et al., 2014; Ding, 2016; Ding et al., 2017; Ogweno and Cramer, 2017; Worden et al., 2012). These relations are generally region-dependent and have large scatter (Caprio et al., 2015). In this section, we propose a new approach in deriving intensity-PGA relation based on the newly collected empirical and analytical fragility database. For each building type and each damage limit state, an empirical fragility curve (exceedance probability vs. macro-seismic intensity) and an analytic fragility curve (exceedance probability vs. PGA) are available, as derived from the median fragilities in Sect. 4~~.1~~. By eliminating the same fragility value, we can derive the corresponding pair of macro-seismic intensity and PGA. Thus, for a series of fragility values, we can further regress the corresponding intensity-PGA relation based on the paired intensities and PGAs. Ideally, we would expect the overlap of all these regressed intensity-PGA relations, regardless of the difference in building type, seismic resistance level and damage state.

5.1 Difference between this new approach and previous practices

Compared with this new approach in intensity-PGA relation development, previous practices directly regressed intensity and PGA datasets within the same geographical range, but no further classification of datasets was conducted, as based on building type or damage state in this study. The lack of further classification of PGA and intensity datasets may explain why the previously derived intensity-PGA relations generally have high scatter. The reason lies behind is that, although macro-seismic intensity is a direct macro indicator of building damage, higher instrumental ground motion (e.g., PGA) does not necessarily mean higher damage to all buildings. Instead, damage is more determined by the seismic resistance capacity of different building types. Thus, further division of intensity and instrumental ground motion records based on affected building types should promisingly help decrease the scatter of regressed intensity-PGA relation.

Furthermore, local site effect also contributes to the amplification of instrumental peak ground motions (PGA or SA), when combining intensity and PGA datasets from areas with different geological background together. This

in turn increases the scatter of regressed intensity-PGA relation. In this regard, it is worth to emphasize that, in our PGA-related analytical fragility database, the PGA parameter is not the real instrumental records as used in regressing traditional intensity-PGA relation, but the input PGA records used in experimental fragility analysis (push-over analysis, incremental dynamic analysis, dynamic history analysis etc.). Therefore, the regional dependence (here we mainly refer to site condition), which contributes to the scatter of traditional PGA-intensity relation, is not a source of uncertainty in our relation.

5.2 Derivation of initial intensity-PGA relation

As a tentative approach, here we derive the relation between intensity and PGA using median fragility as the bridge for each damage limit state of each building type. We're deeply aware that uncertainty is inherent in every single step both in empirical and analytical fragility analysis. However, the trial of using the median fragility as the bridge to develop intensity-PGA relation proposed here, more importantly, aims at providing a new approach in this regard compared with traditional practice, not to backwards reduce the uncertainties (due to differences in building structure, seismic demand inputs, computation methods etc.) in deriving empirical and analytical fragility. By using Eq. (3) for PGA-fragility and intensity-fragility respectively and eliminating fragility as variable, we find:

$$\ln(PGA) = \alpha + \beta * Int,$$

$$with\ \alpha = \ln(\mu_{PGA}) - \frac{\sigma_{PGA}}{\sigma_{Int}} * \mu_{Int,}\ \beta = \frac{\sigma_{PGA}}{\sigma_{Int}} \quad (4)$$

In which, the parameters μ_{PGA}, μ_{Int}, σ_{PGA}, σ_{Int} are taken from Table 4 with values varying across building types and damage limit states.

These intensity-PGA relations are plotted in Fig. 9 (grouped by building types) and Fig. 10 (grouped by damage limit states). Theoretically, higher damage states can occur only for higher intensities or PGA values. For instance, a LS4 damage state at intensity III would not happen, as reflected by the curves in Fig. 9 and Fig. 10: LS1 have the lowest PGA or intensity starting point, while LS4 has the highest. Thus, we plot the intensity-PGA curves for fragility values above 1%. Ideally, we would expect the overlap of all relation curves between intensity and PGA, whether grouped by building type or by damage state. As a matter of fact, for building type "Masonry_A" and "Masonry_B" in Fig. 9, the four intensity-PGA curves of four damage limit states coincide very well. Meanwhile, the discrepancy in intensity-PGA relations of "RC_A" for damage states LS1, LS2, LS3 in Fig. 9 is not surprising, given the relatively high scatter in the original analytical fragility datasets of "RC_A" (as discussed in Sect. 4.~~1~~ and verified by Appendix Fig. ~~A1~~A3-A4).

5.3 Source of abnormality in intensity-PGA curves

For building type "RC_A" and "RC_B" in Fig. 9, it is clear that for the same intensity levels, the corresponding PGA values of damage state LS4 are much higher than that of damage limit states LS1, LS2, LS3. For fixed fragility value, this may due to the underestimation of intensity by the median empirical fragility curve in Fig. 7, or the overestimation of PGA by the median analytical fragility curve in Fig. 8, or a combination of both effects. In this regard, damage data scarcity at higher damage limit states may contribute to the abnormal high PGA

values of LS4. When reviewing the fragility data collection process, it is clear that the construction of empirical fragility database requires the combination of damage statistics from multiple earthquake events that cover a wide range of ground motion levels. Generally, large magnitude earthquakes occur more infrequently in densely populated areas, thus damage data tend to cluster around the low damage states and ground motion levels. This limits the validation of high damage states or ground motion levels (Calvi, 2006). According to Yuan (2008), those seriously damaged buildings in earthquake affected area are mainly masonry buildings. Therefore, the cause of the abnormal high PGA values of damage state LS4 for "RC_A" and "RC_B" can be attributed to the relative scarcity of damage data at higher intensity/PGA level, especially for RC buildings.

As to building type "~~masonry~~ Masonry_A" and "~~masonry~~ Masonry_B" in Fig. 9, for the same intensity level, the PGA values revealed by four damage states of "~~masonry~~ Masonry_B" are generally higher than that in "Masonry_A". This can be more clearly seen from Fig. 10, in which the intensity-PGA relations are grouped by damage limit states~~. How to explain this abnormal phenomenon that given the same intensity level,~~ and the PGA values revealed by "Masonry_B" are generally higher than by all the other three building types~~?~~. To better understand this abnormality, we need to refer to the building seismic resistance level assignment process in this study. In fact, compared with "Masonry_A", buildings assigned as type "Masonry_B" generally have much higher seismic resistance capacity. As aforementioned in Sect. 3.1, ~~In this study,~~ level "A" refers to buildings ~~assigned as~~with pre/low/moderate-code seismic resistance capacity, and level "B" refers to buildings ~~assigned as~~with high-code seismic resistance capacity~~(*building classification details can be found on the online supplementary material*)~~. That is, according to the grouping criteria in Table 3, buildings assigned as "Masonry_B" mainly refer to those built after 2001 with seismic resistance level VIII and above. This is obviously a very high code standard (*more building classification details can be found on the online supplementary material*). Thus, for the same ground motion level, the damage posed on "Masonry_B" should be much slighter than on "Masonry_A". ~~Therefore, for the same PGA level~~Consequently, the corresponding intensity revealed by "~~mansory~~Masonry_B" should be lower than by "~~mansory~~Masonry_A".

~~Actually~~ Currently in mainland China, the macro-seismic intensity level in post-earthquake filed surveys is determined by damage states of three reference buildings types, namely (1) Type A: wood-structure, soil/stone/brick-made old building; (2) Type B: single- or multi- storey brick masonry without seismic resistance; (3) Type C: single- or multi- storey brick masonry sustaining shaking of intensity degree VII. While in this study, buildings assigned as "Masonry_B" mainly refer to those constructed after 2001 with seismic resistance level VIII and above, and their seismic resistance capability is obviously much higher than all those three referred Type A/B/C building types. Therefore, intensity levels derived from damage to those less fragile "Masonry_B" buildings tend to be underdetermined. This may help explain why for the same intensity level, the corresponding PGA revealed by intensity-PGA relation of "~~mansory~~Masonry_B" is higher than that of "~~mansory~~Masonry_A".

Based on above discussion and the initial analysis in Sect. 4~~.1~~, it ~~is clear~~can be summarized that (a) Due to the high scatter in originally collected fragility database ~~(as validated by the low values in Table 4)~~, the intensity-PGA relations derived for LS1, LS2, LS3 of building type "RC_A" are of low robustness (as validated by the low R^2 values in Table 4); (b) Due to the damage data scarcity at high damage states or ground motion levels, intensity-PGA relations for LS4 of "RC_A" and LS4 of "RC_B" are also not fully reliable; (c) Due to the high

seismic resistance capability attached to "Masonry_B", the intensity-PGA relations derived for all four damage limit states of "Masonry_B" have the probability to underestimate intensity (or overestimate PGA) compared with "Masonry_A". Therefore, intensity-PGA curves derived for "Masonry_A" are of relatively highest robustness/reliability. Actually, the four intensity-PGA curves of "Masonry_A" do coincide very well as expected (Fig. 9). According to Yuan (2008), those seriously damaged buildings in earthquake affected areas are also mainly masonry buildings. Therefore, we consider the median empirical and analytical fragility curves derived for "Masonry_A" (with uncertainties ~~shown~~ provided in Appendix Fig. ~~A1~~A3-A4 and Table B1) are ~~also~~ the most representative ones for seismic prone areas in mainland China, compared with those developed for other buildings types in this study.

5.4 Average intensity-PGA relation derived for "Masonry_A"

According to the analysis in Sect. 5.3, intensity-PGA curves derived for four damage limit states of "Masonry_A" are of relatively highest robustness ~~and have no such intensity underestimation probability as "Masonry_B"~~. Therefore, we first focus only on building type "Masonry_A" and average its four curves for discrete intensity values, to derive the corresponding averaged PGA values, as listed in Table 5. If we match the data points in Table 5 with a linear relation between intensity and ln(PGA), we find Eq. (5):

$$\ln(PGA) = 0.521 * Int - 5.43 \pm \varepsilon \qquad (PGA: \mathrm{g}) \tag{5}$$

where ε follows the normal distribution, with 0 as the median value and the standard deviation is σ.

By integrating the uncertainty in both original empirical and analytical fragility data of "Masonry_A" (as shown in Appendix Fig. ~~A1~~A3-A4 and Table B1) into the intensity-PGA relation, the averaged standard deviation σ in Eq. (5) is estimated to be 0.3 (*the detailed uncertainty transmission methodology is given in Appendix C*). As the "Masonry_A" type is the most common and relevant with buildings damaged in historical earthquakes (~~Sect. 5.3~~Yuan, 2008), we recommend using Eq. (5) for building damage assessment for earthquakes occurred in mainland China, especially in seismic active provinces e.g. Sichuan and Yunnan (Fig. 2).

5.5 Comparison with other intensity-PGA relations

Based on the ~~analysis~~ summarization in Sect. 5.3, if we only remove those obviously unreliable intensity-PGA curves, namely LS1, LS2, LS3, LS4 of "RC_A" and LS4 of "RC_B", the range of median PGA values corresponding to each intensity degree can be derived from the remaining intensity-PGA relations, as~~are~~ shown in Table 6. For comparison, the recommended PGA range for each intensity degree in the Chinese ~~Official~~ Seismic Intensity Scale (~~GB17742-~~GB/T 17742-2008) is listed in Table 7. The PGA values for intensity VI, VII in our results are higher than those in ~~GB17742-~~GB/T 17742-2008; while for intensity VII, IX and X, the PGA values are quite comparable. We also found that the recommended PGA ranges in ~~GB17742-~~GB/T 17742-2008 are indeed the same as those given in ~~GB17742-~~GB/T 17742-1980, which was issued in the 1980s around four decades ago. At that time, available damage ~~data~~ information used to derive the intensity-PGA relation in China was quite scarce. Therefore, damaging earthquakes occurred in the United States before 1971 were also largely used, which may not be representative of the situation in China today. Thus, one possible explanation for the relatively low PGAs for low intensity levels (VI, VII) in Table 7 (~~GB17742-~~GB/T 17742-1980/2008) is that, the buildings in the 1980s were more fragile than nowadays buildings. Since macro-seismic intensity is a direct

macro indicator of building damage, nowadays buildings generally have better seismic resistance capacity and thus require higher ground motion (PGA) than buildings in the 1980s to be equally damaged.

Since the recommended PGA ranges in ~~GB17742-~~GB/T 17742-2008 are not so representative of the current building status in mainland China, comparisons with the latest intensity-PGA relation developed in Ding et al. (2017) are also conducted. Ding et al. (2017) adopted traditional practice in regressing the macro-seismic intensities and instrumental PGA records within the same geographical range, by using records for 28 M≥5 earthquakes occurred during 1994-2014 in mainland China. The PGA values for intensity VI-IX in Ding et al. (2017) are listed in Table 8. When comparing our results in Table 5 and Table 6 with that in Table 8, PGA values are quite consistent for both low intensity (VI, VII) and high intensity (VIII, IX) levels, although these data are separately developed by our new approach and by traditional practice. This congruence shows the reasonability of our new approach proposed here in developing intensity-PGA relation.

6 Conclusion

We established empirical fragility database by evaluating 69 papers and theses, mostly from the Chinese literature, that document observations of macro-seismic intensities reflecting earthquake damage occurred in densely populated areas in mainland China over the past four decades. These publications provide empirical fragilities dependent on macro-seismic intensities for four damage limit states (LS1, LS2, LS3, LS4) of four building types (Masonry_A, Masonry_B, RC_A, RC_B). We also established analytical fragility database by scrutinizing 18 papers and theses with results on modeling fragilities for the nominally same building types and the same damage states either by response spectral methods or by time-history response analysis. These analytic methods provide fragilities as functions of PGA. From this wealth of data, we derived the median fragility curves for these building types by removing outliers using box-plot method. ~~Based on the newly collected empirical and analytical fragility database, possible comparisons with several international projects including PERPETUATE, SYNER-G, PAGER, HAZUS, GEM were also conducted.~~

We proposed a new approach by using fragility as the bridge and derived intensity-PGA relations independently for each building type and each damage state. The potential sources of abnormalities in these newly derived intensity-PGA relations were discussed in detail. Ideally the individual intensity-PGA curves should all coincide and allow us to derive an average relation between intensity and PGA. The coincidence is not 100% perfect and deviations for the cases where they occu~~r~~r were discussed. Given the high damage data abundance and wide distribution of masonry buildings in mainland China, for studies referring to historic earthquakes and their losses in seismic active regions, e.g. Sichuan and Yunnan, we recommend utilizing the intensity-PGA relation derived from “Masonry_A” buildings in Eq. (5).

However, for engineering application, due to the scatter~~ing~~ in original fragility datasets and the simplification in using median fragility to derive intensity-PGA relation in our proposed new approach, the use of the preliminary intensity-PGA relations developed here should be with caution. It’s also worth to note that, buildings used for empirical intensity determination and for analytical studies do not coincide: a “Masonry_A” building in a post-event field survey may encompass a wider range than in an analytic study. Therefore, following the novel idea of using fragility as the bridge to develop intensity-PGA relation in this study, possible extensions in the future can

be performing fragility analysis for more specifically designed building types that are more representative of those widely damaged building types in the fields.

Appendix

In Fig. A1, the comparison of Chinese Seismic Intensity Scale with other internationally adopted scales is presented. Additionally, the correspondence relation between intensity and PGA/PGV range suggested by the current seismic intensity scale in China (GB/T 17742-2008) is also graphically presented in Fig. A2. To better illustrate the scatter of the original fragility datasets we collected, ~~error bar analysis was performed and shown in Fig. A1 (empirical data) and Fig. A2 (analytical data) for all building types and seismic resistance levels. Specifically, to better scale the scatter,~~ standard deviations of ~~fragility, namely the exceedance probability of each damage limit state~~ fragility series are also ~~provided~~ plotted in Fig. A3 (empirical data) and Fig. A4 (analytical data)~~, respectively~~. ~~Comparisons with fragility curves extracted from international projects including SYNER-G and HAZUS for masonry buildings are plotted in Fig. A5-A7.~~

In Table B1, more statistical details about our newly constructed fragility datasets, including the number of fragility data before and after removing the outliers, median fragility values used in deriving fragility curve ~~in Fig. 7 and Fig. 8~~ and the standard deviation of each fragility dataset for each building type and each damage state in Fig. 7 and Fig. 8 are listed. Table B2 provides a non-official English translation of China seismic intensity scale: ~~GB17742-~~GB/T 17742-2008, which is modified after CSIS (2019).

Appendix C provides the methodology in transmission of uncertainty from empirical/analytical fragility database to intensity-PGA relation in Eq. (5).

Code/Data availability

More fragility extraction and building classification details are available from online supplement in:
(Filename: *Supplementary_building_classification_details.pdf*).
The earthquake catalog in plotting Fig. 2 is in:
(Filename: *EQ_list_with_field_survey.xlsx*).
The empirical and analytical fragility data in Fig. 3 and Fig. 4 are available in:
(Folder name: *data_Fig3-4*).

Author contribution

JD proposed the idea to review the fragility literature for buildings in mainland China. DX conducted the review work and proposed the new approach in deriving intensity-PGA relation and wrote the ~~text content~~manuscript. FW proposed the methodology of uncertainty transmission from fragility to intensity-PGA relation. All authors joined the revision of the manuscript.

Competing interests

The authors declare that they have no conflict of interests.

Formatted: Font: Not Bold

Formatted: Not Highlight

Formatted: Font: Italic

References

In English:

Antoniou, S. and Pinho, R.: Development and verification of a displacement-based adaptive pushover procedure, Journal of Earthquake Engineering, 8, 643-661, https://doi.org/10.1080/13632460409350504, 2004.

Bilal, M. and Askan, A.: Relationships between Felt Intensity and Recorded Ground-Motion Parameters for Turkey, Bulletin of the Seismological Society of AmericaB SEISMOL SOC AM, 104, 484-496, https://doi.org/10.1785/0120130093, 2014.

Billah, A. H. M. M. and Alam, M. S.: Seismic fragility assessment of highway bridges: A state-of-the-art review, Structure and Infrastructure Engineering, 11, 804-832, https://doi.org/10.1080/15732479.2014.912243, 2015.

Barosh, P. J.: Use of seismic intensity data to predict the effects of earthquakes and underground nuclear explosions in various geologic settings, U.S. Government Printing Office, 1969.

Calvi, G. M., Pinho, R. and Magenes, G.: Development of seismic vulnerability assessment methodologies over t he past 30 years, ISET Jjournal of Earthquake Technology, 43, 75-104, https://www.researchgate.net/publication/241826044, 2006.

Caprio, M., Tarigan, B. and Worden, C. B.: Ground motion to intensity conversion equations (GMICEs): A global relationship and evaluation of regional dependency, Bulletin of the Seismological Society of America, 105, 1476-1490, https://doi.org/10.1785/0120140286, 2015.

CSIS: China seismic intensity scale, a non-official English translation based on contents in Wikipedia, https://en.wikipedia.org/w/index.php?title=China_seismic_intensity_scale&oldid=812457225, last access: 21 May 2019.

Crowley, H., Colombi, M., Silva, V., Ahmad N., Fardis M., Tsionis G., Papailia A., Taucer F., Hancilar U., Yakut A.,, . and Erberik M.A.: D3.1. Fragility functions for common RC building types in Europe, Pavia, Italy, 223 pp., http://www.vce.at/SYNER-G/files/dissemination/deliverables.html, 2011a.

Crowley, H., Colombi, M., Silva, V., Ahmad N., Fardis M., Tsionis G., Karatoni T., Lyrantazaki F., Taucer F., Hancilar U., . and Yakut A., Erberik M.A.: D3.2. Fragility functions for common masonry building types in Europe, Pavia, Italy, 177 pp., http://www.vce.at/SYNER-G/files/dissemination/deliverables.html, 2011b.

Daniell, J.: Development of socio-economic fragility functions for use in worldwide rapid earthquake loss estimation procedures, Ph.D. Thesis, Karlsruhe Institute of Technology, Karlsruhe, Germany, 2014.

Draper, N. R., Smith, H: Applied Regression Analysis, 3rd ed., John Wiley & Sons, New York, United States, 2014.

Del Gaudio, C., Ricci, P. and Verderame, G. M.: Development and urban-scale application of a simplified method for seismic fragility assessment of RC buildings, Engineering Structures, 91, 40-57, https://doi.org/10.1016/j.engstruct.2015.01.031, 2015.

Dumova-Jovanoska, E.: Fragility curves for reinforced concrete structures in Skopje (Macedonia) region, Soil Dynamics and Earthquake Engineering, 19, 455-466, https://doi.org/10.1016/S0267-7261(00)00017-8, 2000.

EMS1998: European Macro-seismic Scale 1998, European Seismological Commission, sub commission on Engineering Seismology, Working Group, Macro-seismic Scales, Conseil de l'Europe, Cahiers du Centre Européen de Géodynamique et de Séismologie, Vol. 15, Luxembourg, 1998.

Fajfar, P.: A nonlinear analysis method for performance-based seismic design, Earthquake spectraSpectra, 16, 573-592, https://doi.org/10.1193/1.1586128, 2000.

FEMA: HAZUS®MH estimated annualized earthquake losses for the United States, FEMA 366, Washington DC, United States, https://secure.madcad.com/media/fema/FEMA-366-2008.pdf, 2008.

FEMA: Multi-hazard loss estimation methodology: earthquake model (HAZUS-MH-MR3), Technical Report, Washington DC, USA, https://www.fema.gov/media-library/assets/documents/24609, 2003.

Formatted: Font: 10 pt

Formatted: Font: 10 pt

Formatted: Font: 10 pt

Freeman, S. A.: The capacity spectrum method, in Proceedings of the 11th European ~~conference~~ Conference on ~~earthquake~~ Earthquake ~~engineering~~Engineering, Paris, France~~.~~, http://citeseerx.ist.psu.edu/viewdoc/summary?doi=10.1.1.460.2405, 1998.

Freeman, S. A.: Review of the development of the capacity spectrum method, ISET Journal of Earthquake Technology, 41(1), 1–13, http://citeseerx.ist.psu.edu/viewdoc/download?doi=10.1.1.451.9286, 2004.

GEM Fragility Database: https://platform.openquake.org/vulnerability/list?type_of_assessment=1, last access: 30 January 2019.

GEM Vulnerability Database: https://www.ucl.ac.uk/epicentre/resources/gem-vulnerability-database, last access: 30 January 2019.

Gorshkov, G. P. and Shenkareva, G. A.: On the Correlation of Seismic Scales, U.S. Joint Publications Research Service, New York, United States, https://apps.dtic.mil/docs/citations/ADA362451, 1960.

Hariri-Ardebili, M. A. and Saouma, V. E.: Seismic fragility analysis of concrete dams: A state-of-the-art review, Engineering ~~structures~~Structures, 128, 374-399, https://doi.org/10.1016/j.engstruct.2016.09.034, 2016.

HAZUS User & Technical Manuals: https://www.fema.gov/hazus-mh-user-technical-manuals, last access: 30 January 2019.

Kaynia, A. M., Fardis, M. and Pitilakis, K.: D3.12: SYNER-G fragility functions of elements at risk, SYNER-G Deliverable 3.12, Norwegian Geotechnical Institute, Norway, 145 pp., http://www.vce.at/SYNER-G/files/dissemination/deliverables.html, 2013.

Maio, R. and Tsionis, G.: Seismic fragility curves for the European building stock, Brussels: JRC Technical Report, European Commission, http://dx.doi.org/10.2788/586263, 2015.

Medvedev, S. and Sponheuer, W: Scale of seismic intensity (MSK1969), in proceedings of the 4th World Conference on Earthquake Engineering, Chilean Association of Seismology and Earthquake Engineering, Santiago, vol 1, 143-153 pp., http://www.iitk.ac.in/nicee/wcee/article/4_vol1_A2-143.pdf, 1969.

Musson, R. M., Grünthal, G. and Stucchi, M.: The comparison of macroseismic intensity scales, Journal of Seismology, 14(2), 413–428, 2010.

Nakamura, H.: Preliminary report on the great Hanshin Earthquake January 17, 1995 (AIJ1995), Japan Society of Civil Engineers, Tokyo, Japan, http://resolver.tudelft.nl/uuid:96f94279-326a-483c-ac1d-c7f9e9226342, 1995.

Ogweno, L. P. and Cramer, C. H.: Improved CENA regression relationships between Modified Mercalli Intensities and ground motion parameters, Bulletin of the Seismological Society of America, 107, 180-197, https://doi.org/10.1785/0120160033, 2017.

PAGER Scientific Background: https://earthquake.usgs.gov/data/pager/background.php, last access: 30 January 2019.

PERPETUATE Project Report Summary: https://cordis.europa.eu/result/rcn/57689_en.html, last access: 30 January 2019.

Pitilakis, K., Crowley, H. and Kaynia, A. M.: SYNER-G: typology definition and fragility functions for physical elements at seismic risk, Geotechnical, Geological and Earthquake Engineering, 27, 432 pp., https://link.springer.com/content/pdf/10.1007/978-94-007-7872-6.pdf, 2014.

Rossetto, T. and Elnashai, A.: Derivation of vulnerability functions for European-type RC structures based on observational data, Engineering ~~structures~~Structures, 25, 1241-1263, https://doi.org/10.1016/S0141-0296(03)00060-9, 2003.

Rota, M., Penna, A. and Magenes, G.: A methodology for deriving analytical fragility curves for masonry buildings based on stochastic nonlinear analyses, Engineering Structures, 32, 1312-1323, https://doi.org/10.1016/j.engstruct.2010.01.009, 2010.

Formatted: Font: (Default) Times New Roman

Silva, V., Crowley, H. and Colombi, M.: Fragility function manager tool, in SYNER-G: Typology Definition and Fragility Functions for Physical Elements at Seismic Risk, 385-402 pp., Springer., https://doi.org/10.1007/978-94-007-7872-6_13, 2014.

SYNER-G Project Deliverables: http://www.vce.at/SYNER-G/files/dissemination/deliverables.html, last access: 30 January 2019.

Tang, B., Lu, X., Ye, L. and Shi, W.: Evaluation of collapse resistance of RC frame structures for Chinese schools in seismic design categories B and C, Earthquake. Engineering. and Engineering. Vibration., 10(3), 369, https://doi.org/10.1007/s11803-011-0073-1, 2011.

Vamvatsikos, D. and Cornell, C. A.: Incremental dynamic analysis, Earthquake Engineering & and Structural Dynamics, 31, 491-514, https://doi.org/10.1002/eqe.141, 2002.

Vamvatsikos, D. and Fragiadakis, M.: Incremental dynamic analysis for estimating seismic performance sensitivity and uncertainty, Earthquake Engineering and Structural Dynamics, 39, 141-163, https://doi.org/10.1002/eqe.935, 2010.

Worden, C. B., Gerstenberger, M. C. and Rhoades, D. A.: Probabilistic relationships between Ground-Motion parameters and modified Mercalli intensity in California, Bulletin of the Seismological Society of America, 102, 204-221, https://doi.org/10.1785/0120110156, 2012.

Yepes-Estrada, C., Silva, V., Rossetto, T., D'Ayala, D., Ioannou, I., Meslem, A. and Crowley, H.: The global earthquake model physical vulnerability database, Earthquake. Spectra, 32(4), 2567–2585, https://doi.org/10.1193/011816EQS015DP, 2016.

Yuan, Y.: Impact of intensity and loss assessment following the great Wenchuan Earthquake, Earthquake Engineering and Engineering Vibration, 7(3), 247–254, http://dx.chinadoi.cn/10.1007/s11803-008-0893-9, 2008.

In Chinese:

A, N.: Simplified Prediction Methods of Earthquake Disaster Losses in Hohhot, M.S. Thesis, Inner Mongolia Normal University, Inner Mongolia, China, 45 pp., 2013.

Bie, D., Feng, Q. and Zhang, T.: A Research on Vulnerability of Brick-Concrete Buildings in Fujian Based on Partition of Region Characteristics, Journal of Catastrophe, 25(S0), 254-257, http://dx.doi.org/10.3969/j.issn.1000-811X.2010.z1.054, 2010.

Chang, X., Alimujiang, Y. and Gao, C.: Disaster Loss Assessment and Characteristic of Seismic Hazard of Heshuo Earthquake with Ms5.0 in Xinjiang on Jan 8th, 2012, Inland Earthquake, 26(3), 279-285, http://dx.doi.org/10.3969/j.issn.1001-8956.2012.03.012, 2012.

Chen, H.: Study on Earthquake Damage Loss Assessment of Urban Buildings' Decorations, M.S. Thesis, Institute of Engineering Mechanics, China Earthquake Administration, Harbin, China, 108 pp., 2008.

Chen, X., Sun, B. and Yan, P.: The characteristics of earthquake disasters distribution and seismic damage to structures in Kangding Ms 6.3 earthquake, Earthquake Engineering and Engineering Dynamics, 37(2), 1-9, http://dx.doi.org/10.13197/j.eeev.2017.02.1.chenxz.001, 2017.

Chen, Y., Chen, Q. and Chen, L.: Vulnerability Analysis in Earthquake Loss Estimate, Earthquake Research in China, 15(2), 97-105, 1999.

Chinese Seismic Intensity Scale: GB17742-GB/T 17742-2008, issued by General Administration of Quality Supervision, Inspection and Quarantine of the People's Republic of China (AQSIQ) and Standardization Administration of the People's Republic of China (SAC), Beijing, China, 2008.

Cui, Z. and Zhai, Y.: Research on Effects of Provincial Characteristic on Architecture, Journal of Catastrophe, 25(S0), 271-274, 2010.

Ding, B., Sun, J., Li, X., Liu, Z. and Du, J.: Research progress and discussion of the correlation between seismic intensity and ground motion parameters, Earthquake Engineering and Engineering Vibration, 34(5), 7–20, http://dx.doi.org/10.13197/j.eeev.2014.05.7.dingbr.002, 2014.

Ding, B.: Study on Related Quantitative Parameters of Seismic Intensity Scale, Ph.D. Thesis, Institute of Engineering Mechanics, China Earthquake Administration, Harbin, China, 195 pp., 2016.

Ding, B., Sun, J. and Du, K.: Study on relationships between seismic intensity and peak ground acceleration, peak ground velocity, Earthquake Engineering and Engineering Dynamics, 37(2), 26-36, http://dx.doi.org/%2010.13197/j.eeev.2017.02.26.dingbr.004, 2017.

Fang, W., Wang, J. and SHI, P.: Comprehensive Risk Governance: Database, Risk Map and Web Platform, Science Press, Beijing, China., 2011.

Gan, P.: Research on the Vulnerability and Damage Index of Seismic Building, M.S. Thesis, Institute of Engineering Mechanics, China Earthquake Administration, Harbin, China, 70 pp., 2009.

Gao, H., Bie, D. and Ma, J.: A Research on Vulnerability for Brick-Residence Buildings in Wenchuan Earthquake Areas, World Earthquake Engineering, 26(4), 73-77, 2010.

Ge, M., Chang, X. and Yiliyaer, A.: Direct Economic Loss and Post-earthquake Recovery and Reconstruction Fund Evaluation of Yutian Ms7.3 Earthquake on Feb.12, 2014, Inland Earthquake, 28(2), 104-112, http://dx.doi.org/10.16256/j.issn.1001-8956.2014.02.003, 2014.

Guo, X., Wang, Z. and Duan, C.: Earthquake Damage Assessment Method for Rural Timber Buildings, Building Science, 27(S2), 64-67, http://dx.doi.org/10.13614/j.cnki.11-1962/tu.2011.s2.035, 2011.

Han, X., Wang, Y. and Zeng, J.: The Seismic Damage Assessment of M4.4 Earthquake of Yuncheng Saline Lake District in March 12, 2016, Shanxi Architecture, 43(15), 21-22, 2017.

He, J. and Kang, R.: The Prediction of Seismic Hazard of Multi-Floor Brick Buildings in Weifang Area of Shandong Province, North China Earthquake Sciences, 17(1), 18-28, 1999.

He, J., Pan, W. and Zhang, J.: Study on the Vulnerability of Buildings in Rural Areas of Yunnan Province Based on Seismic Damage Statistics Since 1993, Building Structure, 46(S1), 379-383, 2016.

He, P. and Fu, G.: Initial Research on Seismic Loss Prediction for Cities in Zhujiang Delta, South China Journal of Seismology, 29(4), 114-126, http://dx.doi.org/10.13512/j.hndz.2009.04.015, 2009.

He, S., Wang, Q. and Gong, P.: Seismic Damage Prediction of Rural Houses in Shiyan City, China Earthquake Engineering Journal, 39(S), 195-201, 2017.

He, Y., Li, D. and Fan, K.: Research on the Seismic Vulnerabilities of Building Structure in Sichuan Region, Earthquake Research in China, 18(1), 52-58, http://dx.doi.org/10.3969/j.issn.1001-4683.2002.01.005, 2002.

Hu, S., Sun, B. and Wang, D.: Approach in Making Empirical Earthquake Damage Matrix, Journal of Earthquake Engineering and Engineering Vibration, 27(6), 46-50, http://dx.doi.org/10.13197/j.eeev.2007.06.010, 2007.

Hu, S., Sun, B. and Wang, D.: A Method for Earthquake Damage Prediction of Building Group Based on Building Vulnerability Classification, Journal of Earthquake Engineering and Engineering Vibration, 30(3), 96-101, http://dx.doi.org/10.13197/j.eeev.2010.03.009, 2010.

Hu, Y.: Earthquake Engineering, Seismological Press, Beijing, China, 1988.

Li, J., Li, Y. and Zhou, R.: Characteristics of Surface Rupture and Building Damage by Ms 6.3 Earthquake in Kangding of Sichuan, China, Mountain Research, 33(2), 249-256, 2015.

Li, P.: Research on Evaluation and Comparison of Seismic Performance in China's Rural Residential Buildings, M.S. Thesis, Ocean University of China, Qingdao, China, 106 pp., 2014.

Li, S., Tan, M. and Wu, G.: Disaster Loss Assessment and Building Seismic Damage Characteristic of Atushi Earthquake with Ms5.2 in Xinjiang on March 11th, 2013, Inland Earthquake, 27(4), 341-347, http://dx.doi.org/10.16256/j.issn.1001-8956.2013.04.007, 2013.

Lin, S., Xie, L. and Gong, M.: Methodology for estimating seismic capacity of city building, Journal of Natural Disasters, 20(4), 31-37, http://dx.doi.org/10.13577/j.jnd.2011.0405, 2011.

Liu, H.: Seismic Disaster of Tangshan Earthquake, Seismological Press, Beijing, China, 1986.

Liu, J., Liu, Y. and Yan, Q.: Performance-based Seismic Fragility Analysis of CFST Frame Structures, China Civil Engineering Journal, 43(2), 39-47, http://dx.doi.org/10.15951/j.tmgcxb.2010.02.017, 2010.

Liu, J.: Performance-based Seismic Design and Seismic Vulnerability Analysis for Isolated High-rise Buildings, M.S. Thesis, Guangzhou University, Guangzhou, China, 111 pp., 2014.

Liu, Y.: Research on Vulnerability of RC Frame-core Wall Hybrid Structures Subjected to the Bidirectional Earthquake, M.S. Thesis, Xi'an University of Architecture and Technology, Xi'an, China, 80 pp., 2014.

Liu, Z.: Study on Seismic Fragility of Tall Reinforced Concrete Structures, Ph.D. Thesis, Institute of Engineering Mechanics, China Earthquake Administration, Harbin, China, 184 pp., 2017.

Lv, G., Zhang, H. and Sun, L.: The Vulnerability Analysis of Important Buildings in Langfang City, Journal of Seismological Research, 40(4), 638-645, 2017.

Ma, K. and Chang, Y.: Earthquake Disaster Prediction of Multistorey Masonry Building, Journal of Hefei University of Technology, 22(6), 58-61, 1999.

Meng, L., Zhou, L. and Liu, J.: Estimation of near-fault strong ground motion and intensity distribution of the 2014 Yutian, Xinjiang, Ms7.3 earthquake, Acta Seismologica Sinica, 36(3), 362-371, http://dx.doi.org/10.3969/j.issn.0253-3782.2014.03.003, 2014.

Meng, Z., Guo, M. and Zhao, H.: Seismic Damage Evaluation of the Important Multi-Storey Brick Concrete Buildings in Baoding, Technology for Earthquake Disaster Prevention, 7(4), 397-403, http://dx.doi.org/%2010.3969/j.issn.1673-5722.2012.04.008, 2012.

Meng, Z., Zhao, H. and Guo, M.: Research on Seismic Damage Prediction of the Building Complex in Baoding, Journal of Seismological Research, 36(2), 202-206, http://dx.doi.org/%2010.3969/j.issn.1000-0666.2013.02.011, 2013.

Ming, X., Zhou, Y. and Lu, Y.: Evaluation of Building Features and Seismic Capacity in Northwest Yunnan, Journal of Seismological Research, 40(4), 646-654, http://dx.doi.org/10.3969/j.issn.1000-0666.2017.04.017, 2017.

Piao, Y.: Study on Housing Seismic Vulnerability of Yunnan and Qinghai Province, M.S. Thesis, Institute of Engineering Mechanics, China Earthquake Administration, Harbin, China, 72 pp., 2013.

Qiu, S. and Gao, H.: The Research of Rural Dwelling's Seismic Vulnerability in Qinghai, Technology for Earthquake Disaster Prevention, 10(4), 969-978, http://dx.doi.org/10.11899/zzfy20150415, 2015.

Shi, W., Chen, K. and Li, S.: Hazard Index and Intensity of the 2007 Ning'er, Yunnan, Ms6.4 Earthquake, Journal of Seismological Research, 30(4), 379-383, http://dx.doi.org/10.3969/j.issn.1000-0666.2007.04.012, 2007.

Shi, Y., Gao, X. and Tan, M.: Disaster Loss Assessment of the Minxian-Zhangxian Ms6.6 Earthquake, 2013, China Earthquake Engineering Journal, 35(4), 717-723, http://dx.doi.org/%2010.3969/j.issn.1000-0844.2013.04.0717, 2013.

Song, L., Tang, L. and Yin, L.: Method for Establishing Fragility Matrix of Groups of Buildings in Shihezi City and its Earthquake Disaster Prediction, Inland Earthquake, 15(4), 320-325, http://dx.doi.org/%2010.3969/j.issn.1001-8956.2001.04.005, 2001.

Sun, B. and Chen, H.: Urban Building Loss Assessment Method Considering the Decoration Damage due to Earthquake, Journal of Earthquake Engineering and Engineering Vibration, 29(5), 164-169, 2009.

Sun, B. and Zhang, G.: Statistical Analysis of the Seismic Vulnerability of Various Types of Building Structures in Wenchuan M8.0 Earthquake, China Civil Engineering Journal, 45(5), 26-30, http://dx.doi.org/10.15951/j.tmgcxb.2012.05.015, 2012.

Sun, B., Chen, H. and Yan, P.: Research on Zoned Characteristics of Buildings Seismic Capacity along North South Seismic Belt-take Sichuan Province as an Example, China Civil Engineering Journal, 47(S), 6-10, http://dx.doi.org/10.15951/j.tmgcxb.2014.s1.002, 2014.

Sun, B., Wang, M. and Yan, P.: Damage Characteristics and Seismic Analysis of Single-storey Brick Bent Frame Column Industrial in Lushan Ms7.0 Earthquake, Journal of Earthquake Engineering and Engineering Vibration, 33(3), 1-8, 2013.

Sun, L.: Research on the Earthquake Disaster Loss Assessment Method for Urban Areas and System Development, Ph.D. Thesis, Xi'an University of Architecture and Technology, Xi'an, China, 171 pp., 2016.

Wang, G.: The Performance-based Fragility Analysis of Base-isolated RC Frame Structure, M.S. Thesis, Lanzhou University of Technology, Lanzhou, China, 75 pp., 2013.

Wang, H., Huang, H. and Yu, W.: Analysis on the Regional Building Vulnerability Based on the Damage Influencing Factors, Inland Earthquake, 25(3), 275-282, http://dx.doi.org/10.16256/j.issn.1001-8956.2011.03.001, 2011.

Wang, Y., Shi, P. and Wang, J.: The Housing Loss Assessment of Rural Villages Caused by Earthquake Disaster in Yunnan Province, Acta Seismologica Sinica, 27(5), 551-560, http://dx.doi.org/%2010.3321/j.issn:0253-3782.2005.05.010, 2005.

Wang, D. L., Wang, X. Q. and Dou, A. X.: Primary study on the quantitative relationship between the typical building structures in western China, Earthquake, 27(3), 105-110, http://dx.doi.org/10.3969/j.issn.1000-3274.2007.03.014, 2007.

Wang, Y.: The Research and Manufacture of Urban Buildings Seismic Disasters Prediction Information System Based on ArcGIS, M.S. Thesis, Jiangxi University of Science and Technology, Ganzhou, China, 99 pp., 2007.

Wei, F., Cai, Z. and Jiao, S.: A Fast Approach to Regional Hazard Evaluation Based on Population Statistical Data, Acta Seismologica Sinica, 30(5), 518-524, http://dx.doi.org/10.3321/j.issn:0253-3782.2008.05.010, 2008.

Wen, H., Hu, W. and Tan, M.: Preliminary Analysis on Earthquake Disaster of Building in Two Destructive Earthquakes of Xinjiang, Inland Earthquake, 31(4), 325-334, http://dx.doi.org/10.16256/j.issn.1001-8956.2017.04.001, 2017.

Wenliuhan, H., Zhang, Y. and Wang, D.: Review on Seismic Vulnerability and Economic Loss Assessment of Engineering Structures, Journal of Architecture and Civil Engineering, 32(6), 17-29, http://dx.doi.org/%2010.3969/j.issn.1673-2049.2015.06.003, 2015.

Wu, S.: Seismic Vulnerability Analysis of Masonry Buildings, M.S. Thesis, Institute of Engineering Mechanics, China Earthquake Administration, Harbin, China, 85 pp., 2015.

Xia, S.: Assessment of Seismic Intensity with Mean Damage Index in an Earthquake-resistant Region, M.S. Thesis, Institute of Geophysics, China Earthquake Administration, Beijing, China, 128 pp., 2009.

Xu, W. and Gao, M.: Statistical analysis of the completeness of earthquake catalogues in China mainland, China Journal of Geophysics, 57(9), 2802–2281, http://dx.doi.org/10.6038/cjg20140907, 2014.

Yang, G.: The study of vulnerability analysis of existing buildings under earthquake disaster, M.S. Thesis, Shenyang Jianzhu University, Shenyang, China., 78 pp., 2015.

Yang, X.: Rapid Loss Assessment for Earthquake Disaster Using Seismic Spatial Information Grid, Ph.D., Thesis, Huazhong University of Science and Technology, Wuhan, China, 121 pp., 2014.

Yang, X., Yang, J. and Che, W.: Seismic Vulnerability Study of Buildings in Different Enforcing Zones in Yunnan Province, Value Engineering, 229-232, http://dx.doi.org/10.14018/j.cnki.cn13-1085/n.2017.12.095, 2017.

Ye, Z., Yan, J. and Yang, L.: Study on the Earthquake Damage Characteristics of Tibetan Dwellings in Sichuan Province, Earthquake Research in Sichuan, (4), 24-29, http://dx.doi.org/10.13716/j.cnki.1001-8115.2017.04.007, 2017.

Yin, Z.: Classification of Structure Vulnerability and Evaluating Earthquake Damage from Future Earthquake, Earthquake Research in China, 12(1), 49-55, 1996.

Yin, Z., Li, S. and Yang, S.: Estimating Method of Seismic Damage and Seismic Loss, Earthquake Engineering and Engineering Vibration, 10(1), 99-108, http://dx.chinadoi.cn/10.13197/j.eeev.1990.01.010, 1990.

Yu, X., Lv, D. and Fan, F.: Seismic Damage Assessment of RC frame Structures Based on Vulnerability Index, Engineering Mechanics, 34(1), 69-75, http://dx.doi.org/10.6052/j.issn.1000-4750.2015.09.0731, 2017.

Zeng, Z.: Fragility Analysis and Seismic Reliability of the Isolated Structure, M.S. Thesis, Guangzhou University, Guangzhou, China, 110 pp., 2012.

Zhang, G. and Sun, B.: A Method for Earthquake Damage Prediction of Building Groups Based on Multiple Factors, World Earthquake Engineering, 26(1), 26-30, 2010.

Zhang, J., Pan, W. and Song, Z.: An Assessment of Seismic Vulnerability of Urban Structures Based on the Intensity Gap, Earthquake Engineering and Engineering Dynamics, 37(4), 77-84, http://dx.doi.org/10.13197/j.eeev.2017.04.77.zhangj.009, 2017.

Zhang, Q., Cheng, M. and Niu, L.: Seismic Vulnerability Analysis of Masonry Structures after Earthquake in Panzhihua Area, Architecture Application, (10), 110-112, http://dx.doi.org/10.16001/j.cnki.1001-6945.2016.10.023, 2016.

Zhang, T., Gao, H. and Huang, H.: Study on Regional Factors that Influence the Results of Vulnerability Analysis - A Case Study in Fujian, Journal of Catastrophe, 26(3), 73-77, http://dx.doi.org/%2010.3969/j.issn.1000-811X.2011.03.015, 2011.

Zhang, Y., Kang, J. and Wei, M.: Seismic Damage Evaluation of Building Based on GIS in Changchun, Journal of Northeast Normal University, 46(3), 124-131, 2014.

Zheng, S., Yang, W. and Yang, F.: Seismic Fragility Analysis for RC Core Walls Structure Based on MIDA Method, Journal of Vibration and Shock, 34(1), 117-123, http://dx.chinadoi.cn/10.13465/j.cnki.jvs.2015.01.021, 2015.

Zhou, G., Fei, M. and Xie, Y.: Discussion of the Intensity VIII of the Ms5.8 Yingjiang Earthquake on Mar. 10, 2011, Journal of Seismological Research, 34(2), 207-213, http://dx.chinadoi.cn/10.3969/j.issn.1000-0666.2011.02.017, 2011.

Zhou, G., Hong, L. and Liu, C.: Research on Assessment of Building Direct Economic Loss of Earthquake Based on GIS, Geomatics and Spatial Information Technology, 36(10), 56-59, http://dx.doi.org/10.3969/j.issn.1672-5867.2013.10.017, 2013.

Zhou, G., Tan, W. and Shi, W.: Seismic Hazard Matrix of House Construction in Yunnan, Earthquake Research in China, 23(2), 115-123, http://dx.chinadoi.cn/10.3969/j.issn.1001-4683.2007.02.001, 2007.

Zhou, W. and Wang, S.: Investigation and Vulnerability Analysis of the Dwellings in South Fujian Province, Journal of Fuzhou University, 43(1), 123-128, http://dx.chinadoi.cn/10.7631/issn.1000-2243.2015.01.0123, 2015.

Zhu, J.: Seismic Fragility and Risk Analysis of RC Buildings, Ph.D. Thesis, Xi'an University of Architecture and Technology, Xi'an, China, 153 pp., 2010.

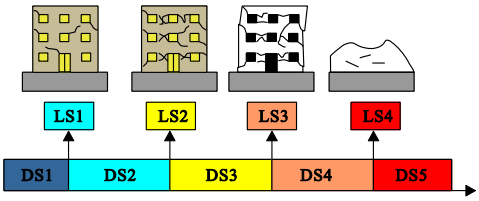

Figure 1: Corresponding Relation between structural damage states (DS1, D2, D3, DS4, DS5) and limit states (LS1, LS2, LS3, LS4) (modified from Wenliuhan et al., 2015).

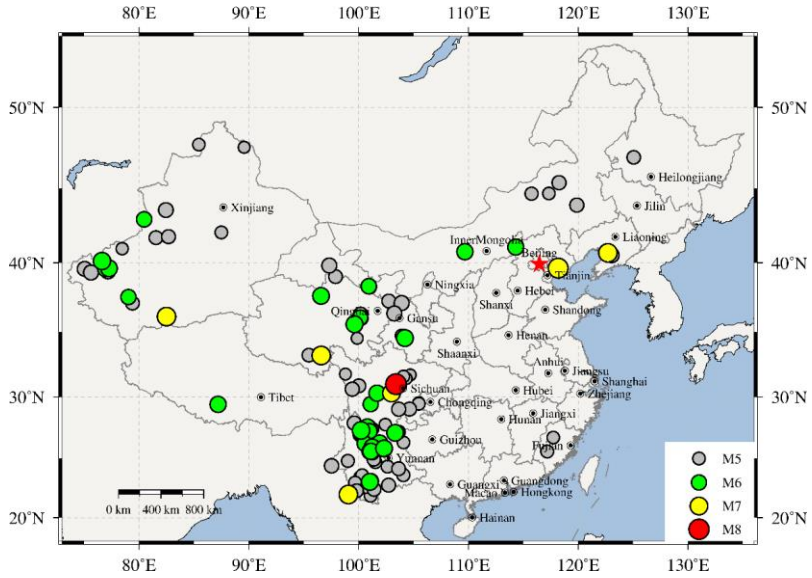

Figure 2: The distribution of earthquakes occurred in mainland China and its neighbouring area, for which field surveys were conducted. Detailed earthquake catalogue can be found from the online supplement, which is newly compiled based on Ding (2016) and Xu et al. (2014).

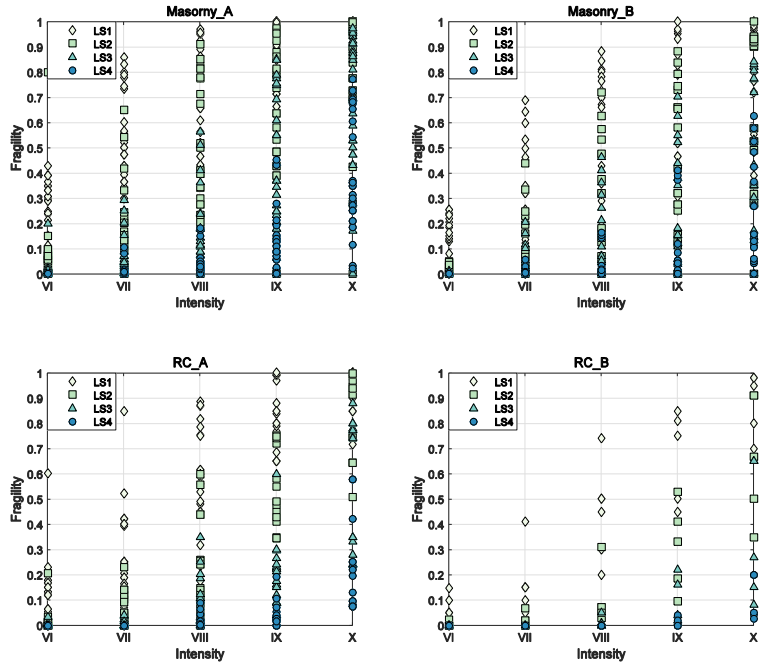

Figure 3: The distribution of empirical fragility data from post-earthquake field surveys, depicting the relation between the exceedance probability of each damage limit state (LS1, LS2, LS3, LS4) at given macro-seismic intensity levels. The fragility datasets are grouped by building types (masonry and RC) and seismic resistance levels (A and B).

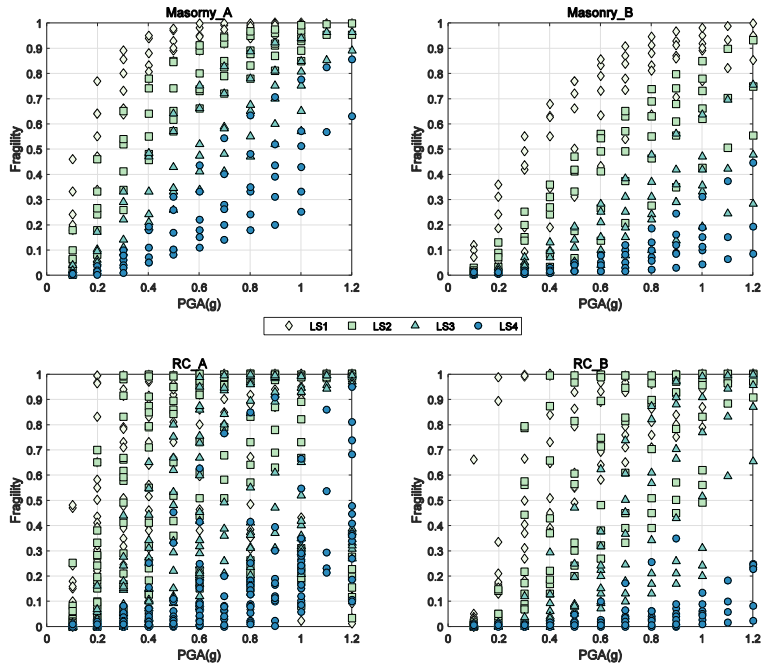

Figure 4: The distribution of analytical fragility data derived from non-linear analyses, depicting the relation between the exceedance probability of each damage limit state (LS1, LS2, LS3, LS4) at given PGA levels. The fragility datasets are grouped by building types (masonry and RC) and seismic resistance levels (A and B).

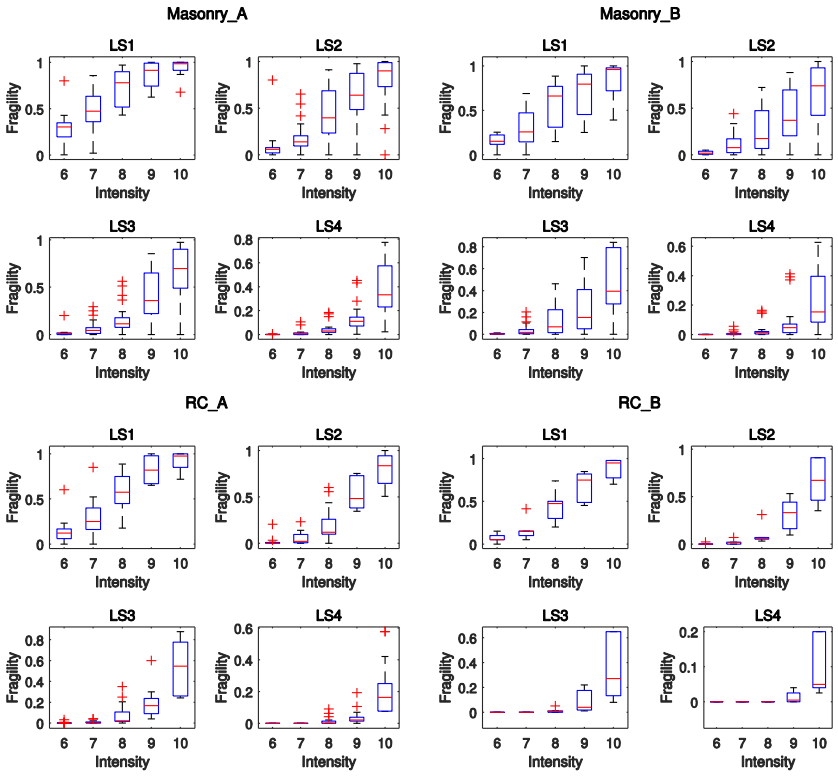

Figure 5: Outlier-check using box-plot method for empirical fragility data. Five macro-seismic intensity levels are used to classify the original fragility datasets: VI, VII, VIII, IX, X. "A" and "B" represent the pre/low/moderate-code and high-code seismic resistance level, respectively (more classification details are available from online supplement). LS1, LS2, LS3, LS4 are the four damage limit states. Outliers are marked by red crosses and red lines within each box indicates the 50% quantile fragility value.

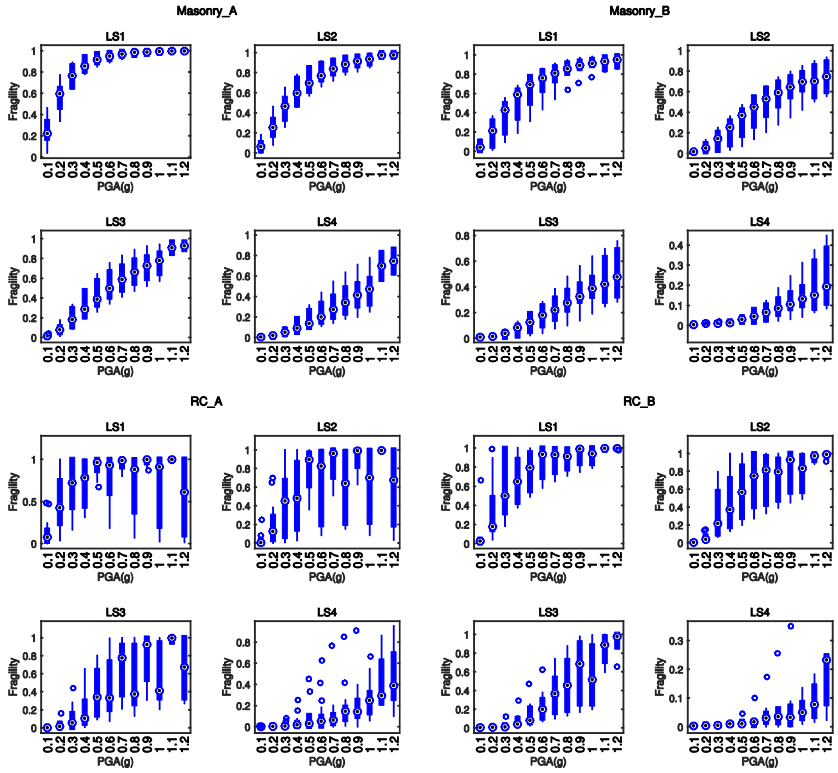
Masonry_A
Masonry_B
RC_A
RC_B
LS1
LS2
LS3
LS4
Fragility
PGA(g)

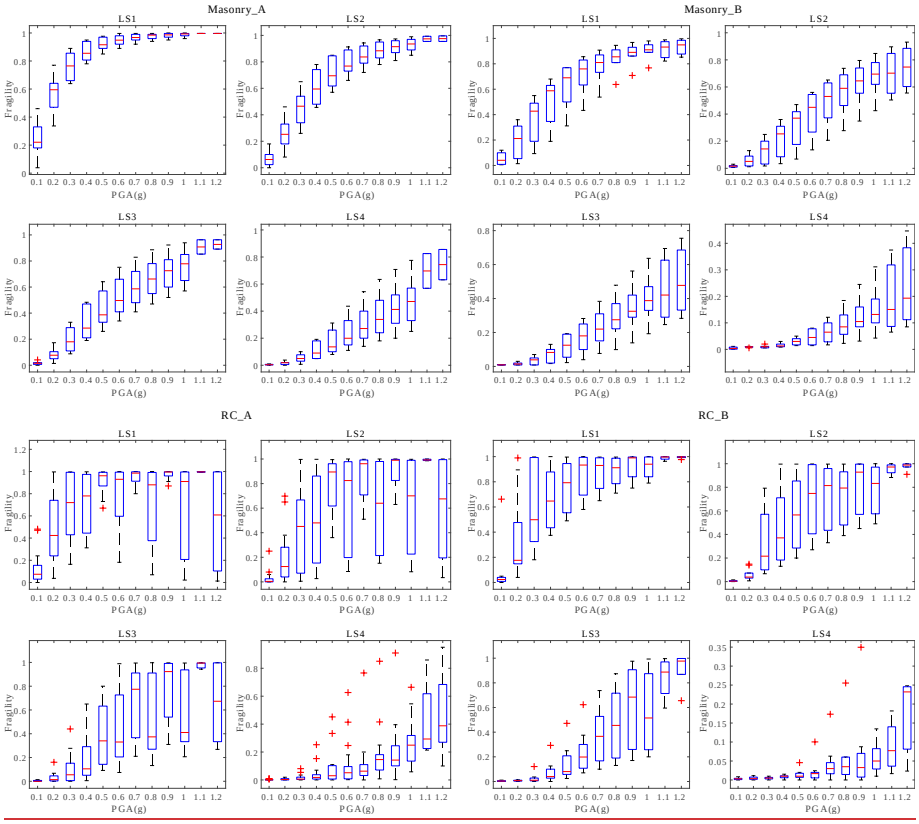

Figure 6: Outlier-check using box-plot method for analytical fragility data. Twelve PGA levels are used to group the discrete analytical fragility datasets: 0.1-1.2 g. "A" and "B" represent the pre/low/moderate-code and high-code seismic resistance level, respectively (more classification details are available from online supplement). LS1, LS2, LS3, LS4 are the four damage limit states. Outliers are marked by red crosses and red line~~blue hollow circles and blue dot~~ within each box indicates the 50% quantile fragility value.

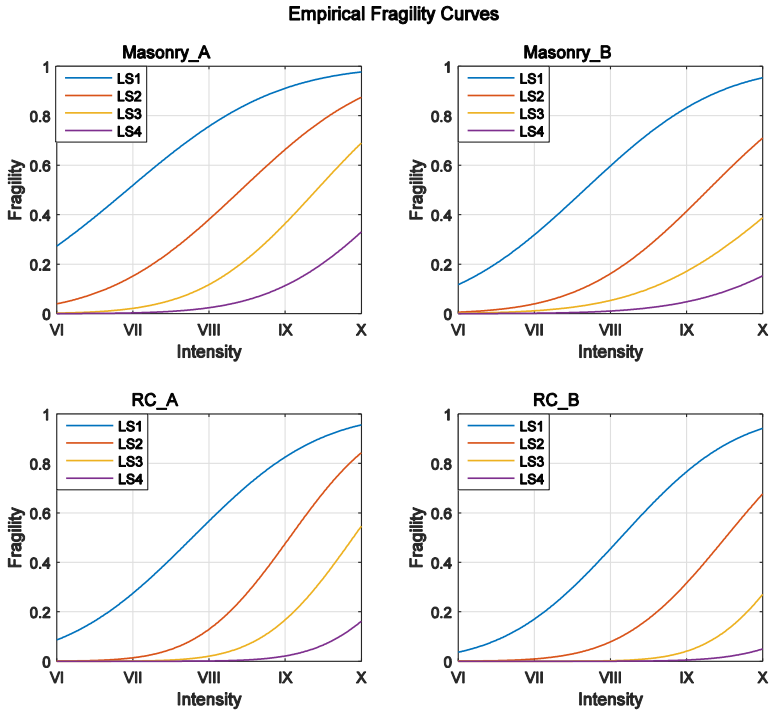
Empirical Fragility Curves
Masonry_A
Masonry_B
RC_A
RC_B
LS1
LS2
LS3
LS4
Fragility
Intensity
0
0.2
0.4
0.6
0.8
1
VI
VII
VIII
IX
X

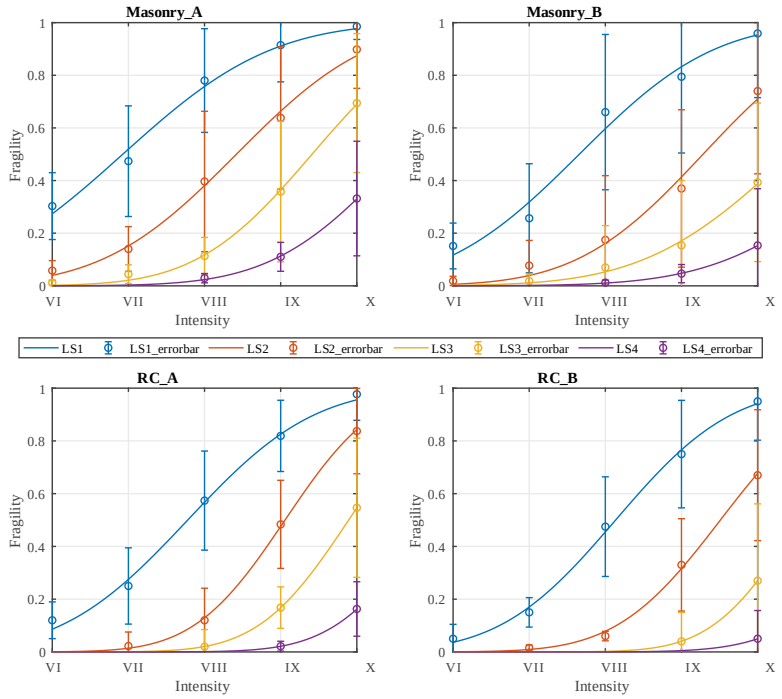

Figure 7: Median fragility curve and error-bar analysis~~s~~ derived from empirical fragility datasets, which depicts the relation between macro-seismic intensity and exceedance probability of each damage limit state (LS1, LS2, LS3, LS4) for masonry and RC building types (Note: these median fragility curves are of varying robustness; see Sect. 4.~~1~~ and Sect. 5.3 for more details). ~~Detailed values are given in Table B1.~~ The circle within each bar represents the median exceedance probability of each damage limit state; the length of each bar indicates the value of the corresponding standard deviation. Only intensity and PGA values with truncated exceedance probability ≥1% for each damage limit state of each building type are plotted, since higher damage states can appear only for higher intensities or PGA values (see Sect. 5.2 for more details). Detailed values of median fragility and standard deviation are given in Table B1.

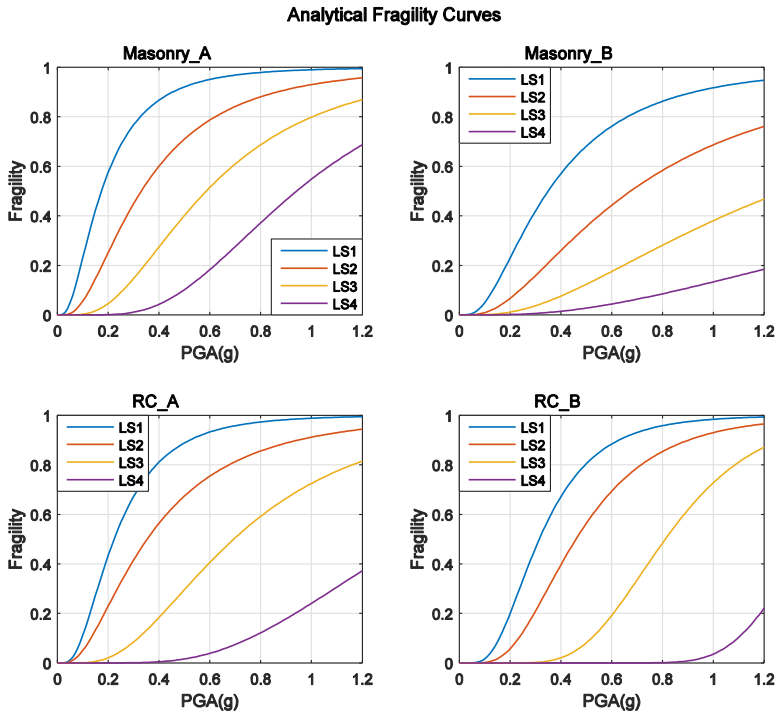
Analytical Fragility Curves
Masonry_A
Masonry_B
RC_A
RC_B
Fragility
PGA(g)
LS1
LS2
LS3
LS4
0
0.2
0.4
0.6
0.8
1
1.2

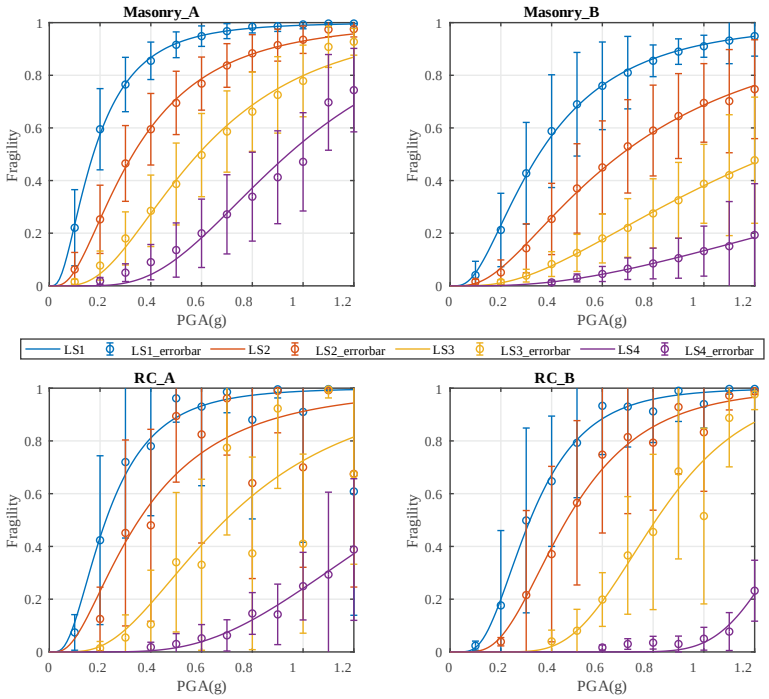

Figure 8: Fragility ~~curves~~ curve and error-bar analysis derived from analytical fragility datasets, which depicts the relation between PGAs (unit: g) and exceedance probability of each damage limit state (LS1, LS2, LS3, LS4) for masonry and RC building types (Note: these median fragility curves are of varying robustness; see Sect. 4.~~1~~ and Sect. 5.3 for more details). ~~Detailed values are given in Table B1.~~ The circle within each bar represents the median exceedance probability of each damage limit state; the length of each bar indicates the value of the corresponding standard deviation. Only intensity and PGA values with truncated exceedance probability >1% for each damage limit state of each building type are plotted, since higher damage states can appear only for higher intensities or PGA values (see Sect. 5.2 for more details). Detailed values of median fragility and standard deviation are given in Table B1.

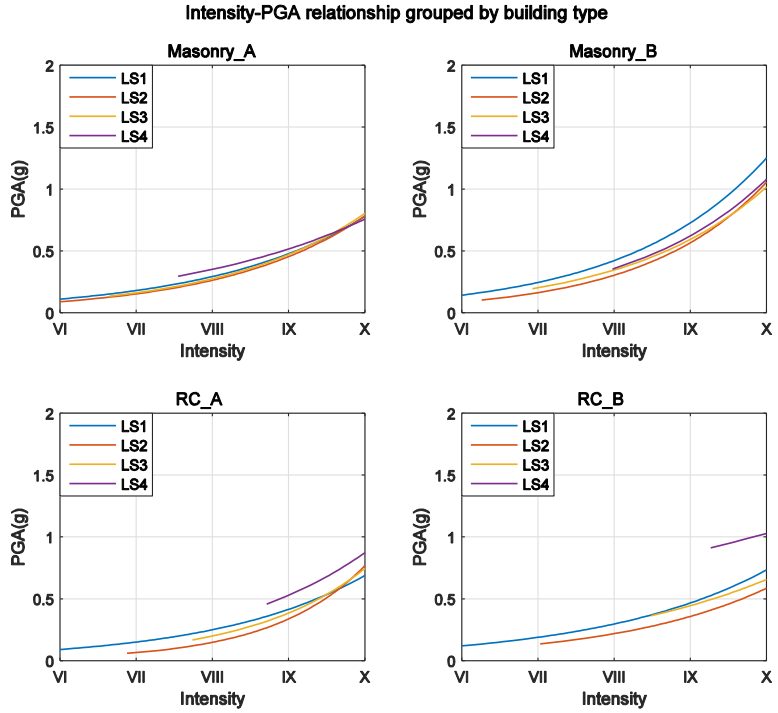

Figure 9: Intensity-PGA relations grouped by building types. Only intensity and PGA values with truncated exceedance probability ≥1% for each damage limit state of each building type are plotted, since higher damage states can appear only for higher intensities or PGA values (see Sect. 5.2 for more details).

5

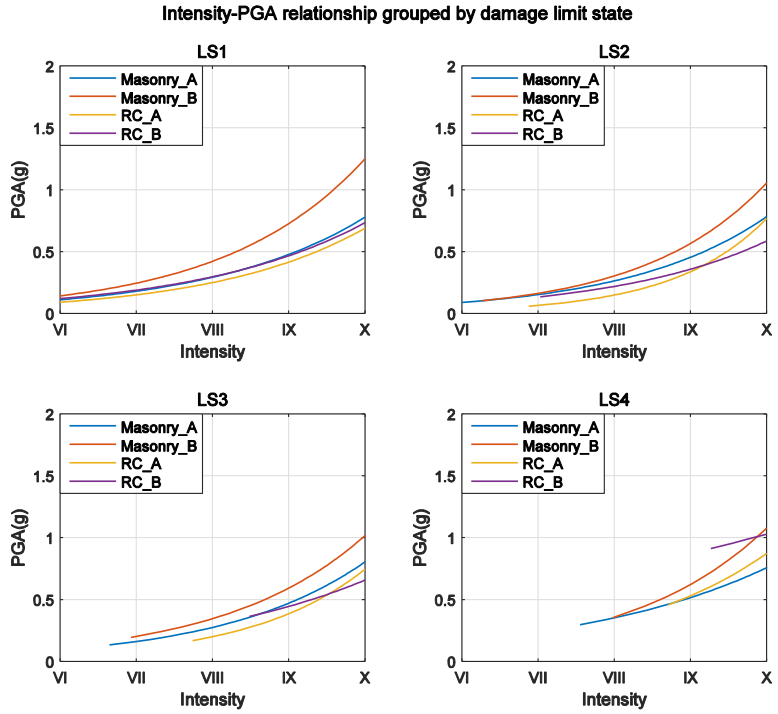

Figure 10: Intensity-PGA relations grouped by damage limit states. Only intensity and PGA values with truncated exceedance probability ≥1% for each damage limit state of each building type are plotted, since higher damage states can appear only for higher intensities or PGA values (see Sect. 5.2 for more details).

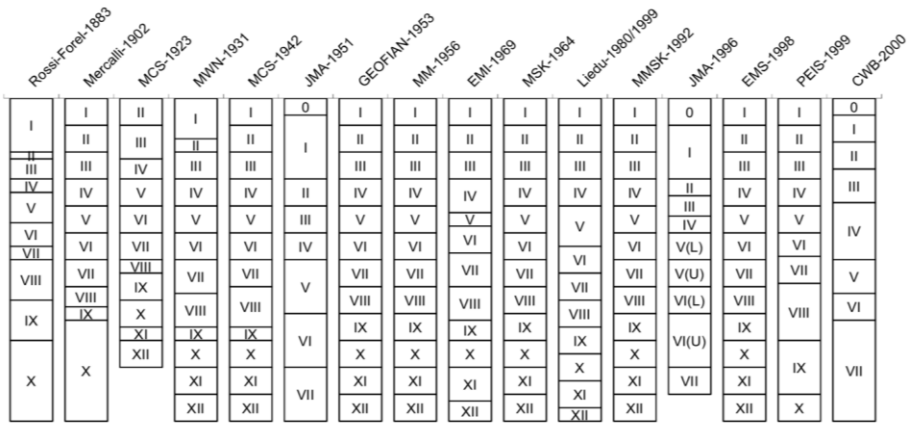

Figure A1: Comparison of Chinese Seismic Intensity Scale with other internationally used seismic scales (Daniell, 2014; after the work of Gorshkov and Shenkareva (1960), Barosh (1969), Musson et al. (2010)). In this figure, "Liedu-1980/1999" represents the Chinese Seismic Intensity Scale, which has marginal change compared with the current intensity scale GB/T 17742-2008 used in China.

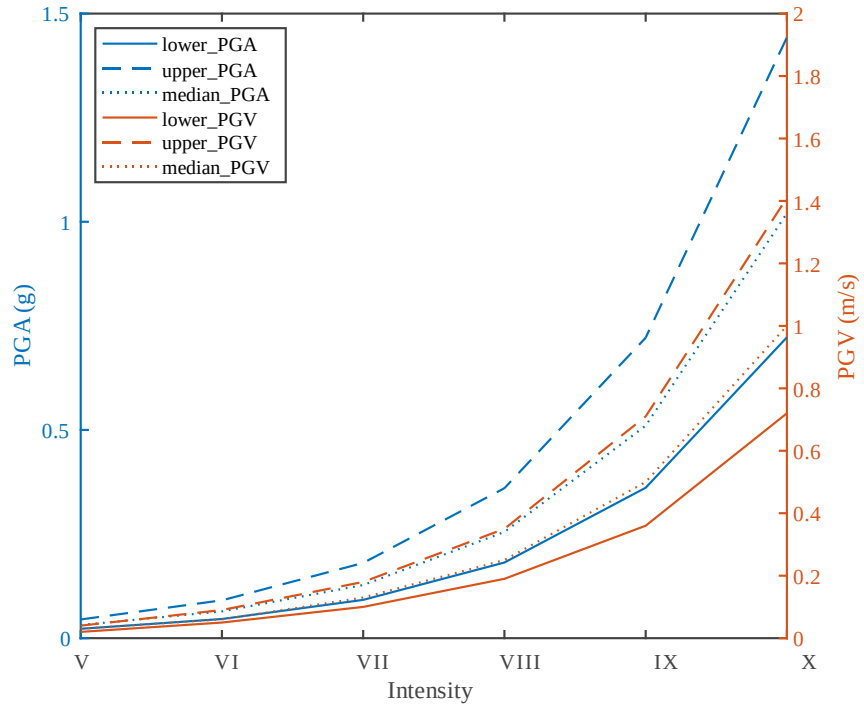

Figure A2: The suggested correspondence relation between intensity and PGA/PGV range by Chinese Seismic Intensity Scale (GB/T 17742-2008).

Formatted: Font: Bold
Formatted: Font: Not Bold
Formatted: Font: Not Bold
Formatted: Font: Not Bold
Formatted: Font: Not Bold
Formatted: Font: Not Bold
Formatted: Font: Not Bold
Formatted: Font: Not Bold
Formatted: Font: Not Bold
Formatted: Font: Bold, Font color: Auto
Formatted: Font: Bold

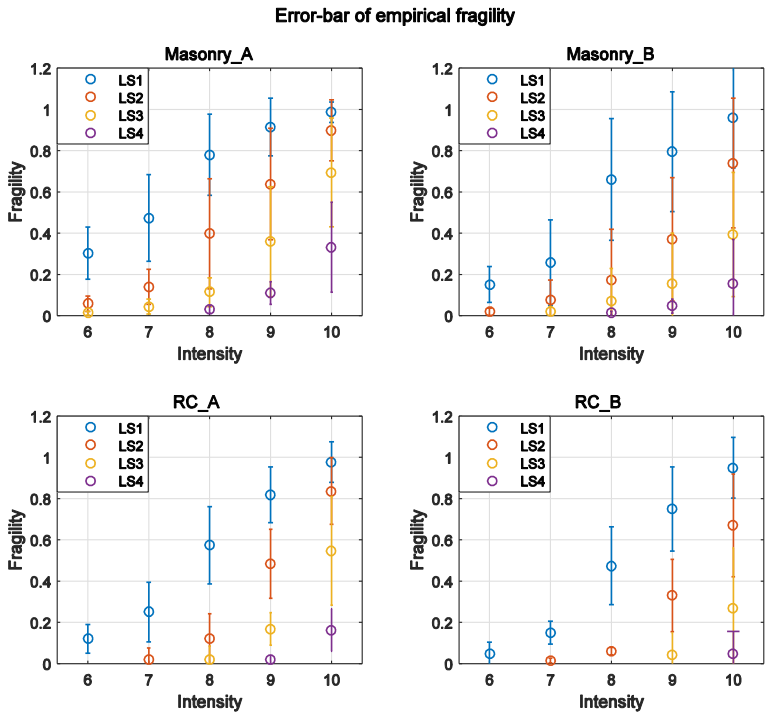

Figure A1: The error-bar of empirical fragility, namely the exceedance probability of each damage limit state (LS1, LS2, LS3, LS4) derived from empirical fragility datasets for each building type (Masonry_A, Masonry_B, RC_A, RC_B). Detailed values are given in Table B1. The circle within each bar represents the median exceedance probability of each damage limit state; the length of each bar indicates the value of the corresponding standard deviation. Only intensity and PGA values with truncated exceedance probability ≥1% for each damage limit state of each building type are plotted, since higher damage states can appear only for higher intensities or PGA values (see Sect. 5.2 for more details).

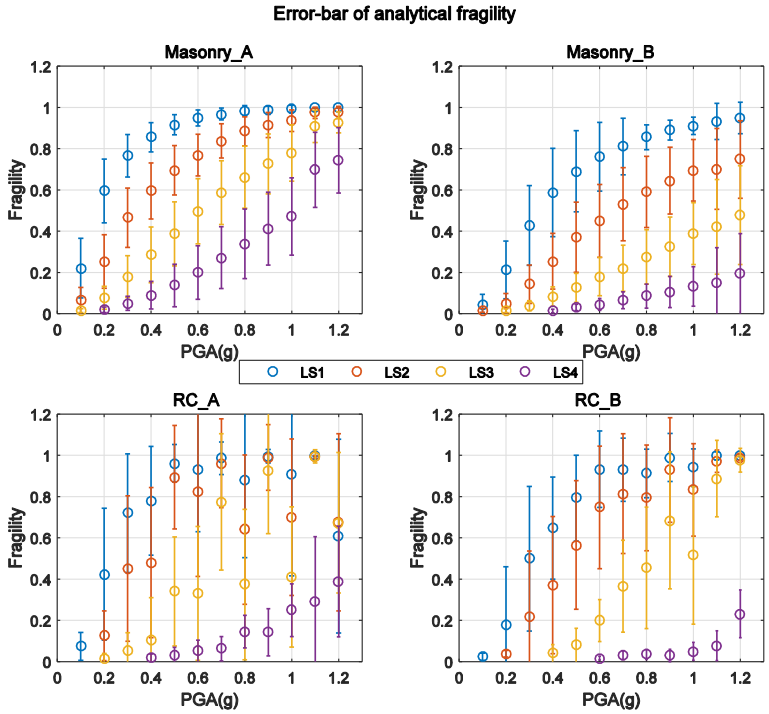

Figure A2: The error-bar of analytical fragility, namely the exceedance probability of each damage limit state (LS1, LS2, LS3, LS4) derived from analytical fragility datasets for each building type (Masonry_A, Masonry_B, RC_A, RC_B). Detailed values are given in Table B1. The circle within each bar represents the median exceedance probability of each damage limit state; the length of each bar indicates the value of the corresponding standard deviation. Only intensity and PGA values with truncated exceedance probability ≥1% for each damage limit state of each building type are plotted, since higher damage states can appear only for higher intensities or PGA values (see Sect. 5.2 for more details).

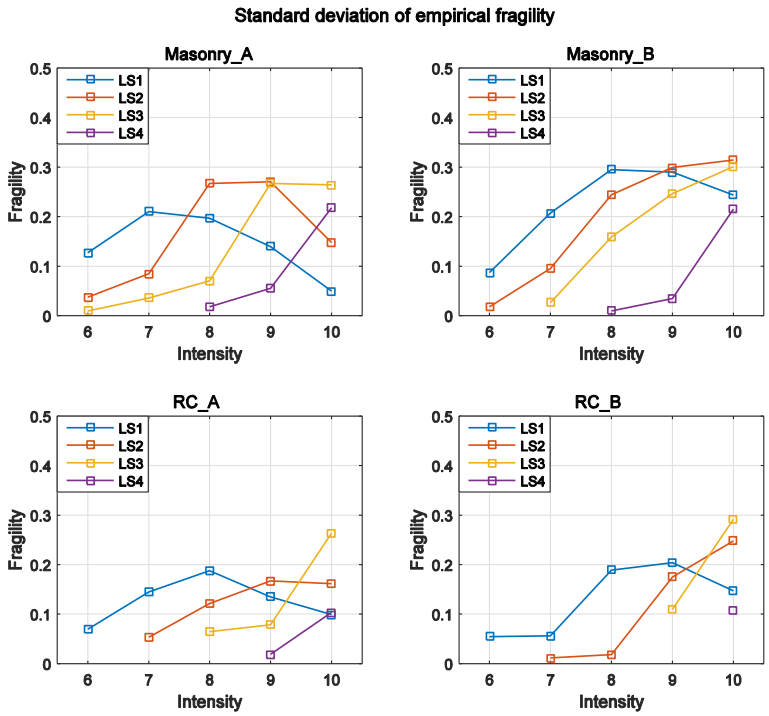

Figure A3: Standard deviation of empirical fragility, namely the exceedance probability of each damage limit state (LS1, LS2, LS3, LS4) derived based on empirical fragility datasets for each building type (Masonry_A, Masonry_B, RC_A, RC_B; detailed values are given in Table B1). Only intensity and PGA values with truncated exceedance probability ≥1% for each damage limit state of each building type are plotted, since higher damage states can appear only for higher intensities or PGA values (see Sect. 5.2 for more details).

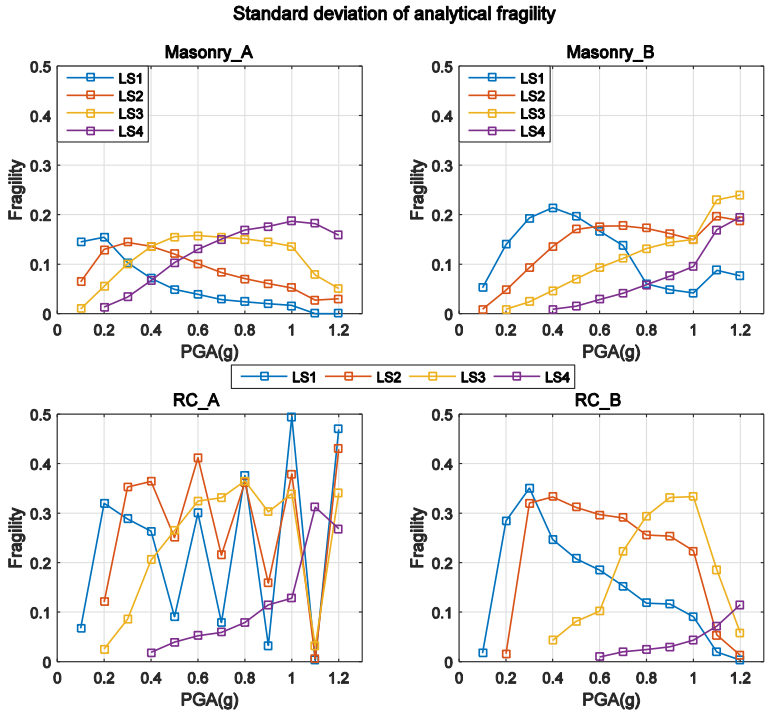

Figure A4: Standard deviation of analytical fragility, namely the exceedance probability of each damage limit state (LS1, LS2, LS3, LS4) derived based on analytical fragility datasets for each building type (Masonry_A, Masonry_B, RC_A, RC_B; detailed values are given in Table B1). Only intensity and PGA values with truncated exceedance probability ≥1% for each damage limit state of each building type are plotted, since higher damage states can appear only for higher intensities or PGA values (see Sect. 5.2 for more details).

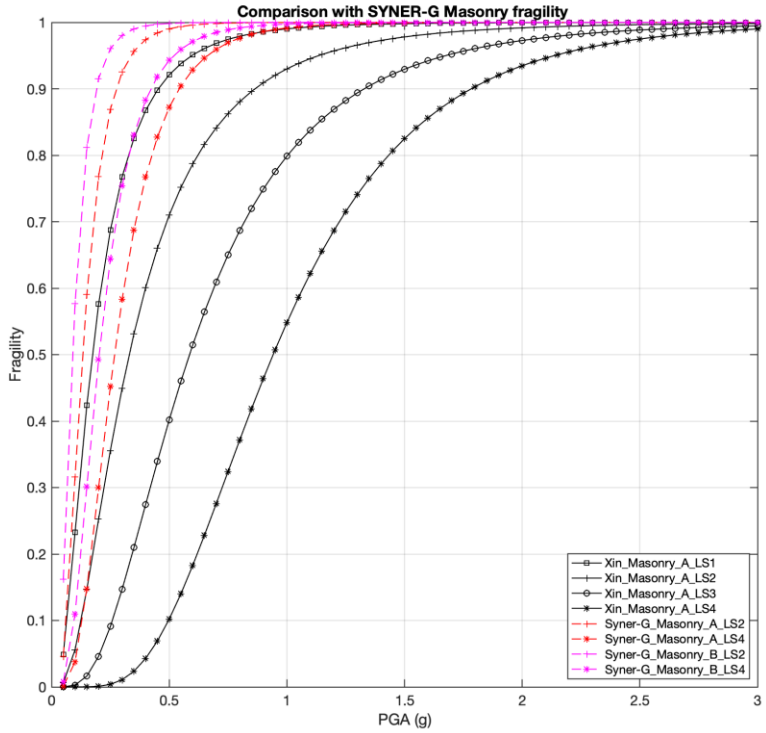

Figure A5: Fragility curve comparison between SYNER-G project mean outputs and our median results for masonry building type. In SYNER-G project, "Masonry_A", "Masonry_B" refer to the low-rise, mid-rise masonry building types, respectively; LS2 and LS4 refer to yielding state and collapse state (see Sect. 4.2.2 for more detailed discussion on sources of discrepancy).

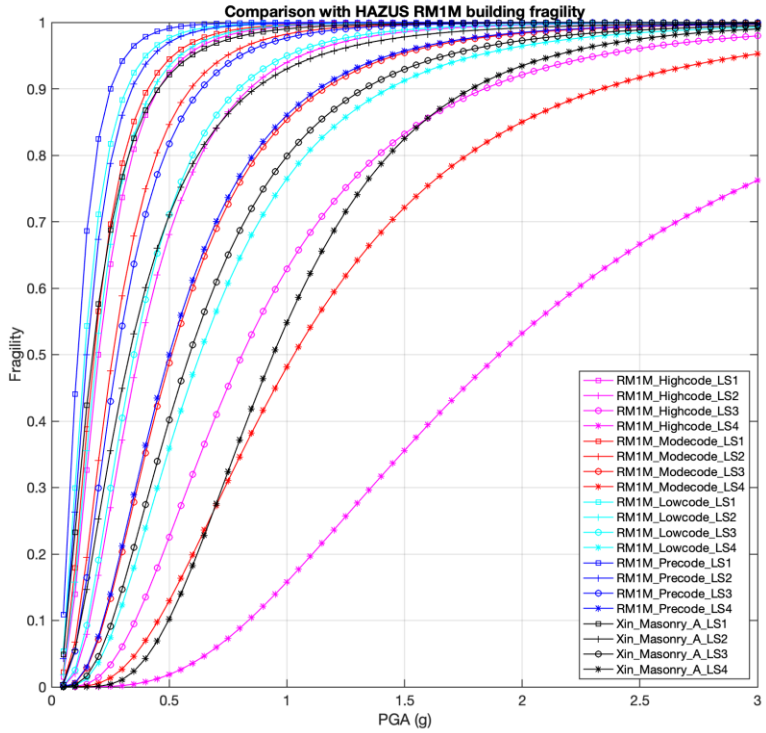

Figure A6: Median fragility curve comparison between HAZUS "RM1M" building type and our work for "Masonry_A". In HAZUS project, "RM1M" refers to "Mid-rise Reinforced Masonry Bearing Walls with Wood or Metal Deck Diaphragms" (see Sect. 4.2.4 for more details).

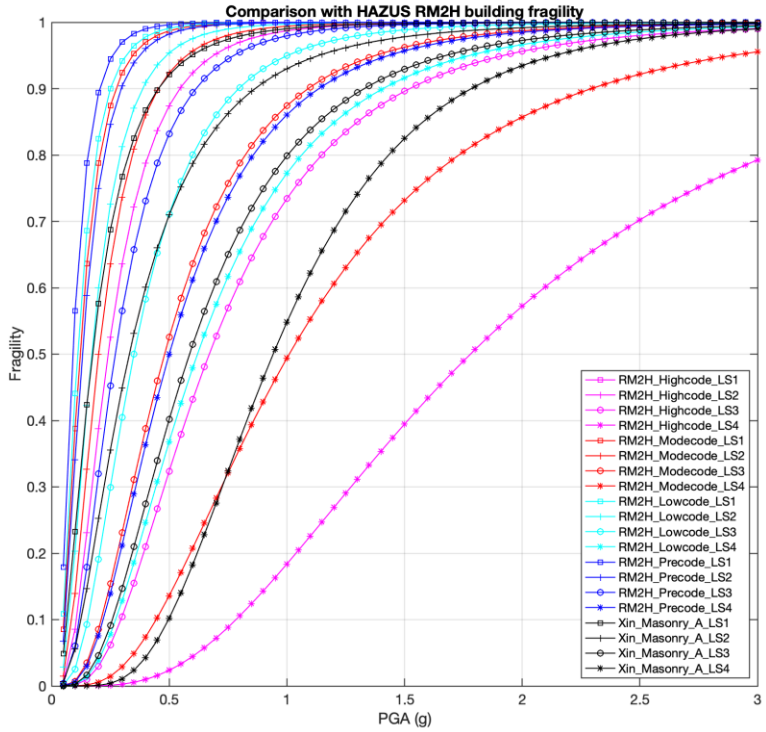

~~**Figure A7:** Median fragility curve comparison between HAZUS "RM2H" building and our work for "Masonry_A". In HAZUS project, "RM2H" refers to "High-rise Reinforced Masonry Bearing Walls with Precast Concrete Diaphragms" (see Sect. 4.2.4 for more details).~~

5

Table 1: Example of major damage states classification methods (modified after Rossetto and Elnashai, 2003).

<table>
<tr><th>vulnerability</th><th>HAZUS1999</th><th>EMS1998</th><th>MSK1969</th><th>AIJ1995</th><th>China2008</th></tr>
<tr><td>0</td><td colspan="5">no damage</td></tr>
<tr><td>10</td><td rowspan="3">slight damage</td><td rowspan="2">Grade 1</td><td rowspan="2">D1</td><td rowspan="2">Light</td><td>D1</td></tr>
<tr><td>20</td><td>D2</td></tr>
<tr><td>30</td><td rowspan="2">Grade 2</td><td rowspan="2">D2</td><td rowspan="3">Minor</td><td rowspan="3">D3</td></tr>
<tr><td>40</td></tr>
<tr><td>50</td><td rowspan="3">moderate damage</td><td rowspan="3">Grade 3</td><td rowspan="3">D3</td></tr>
<tr><td>60</td><td rowspan="2">Moderate</td><td rowspan="3">D4</td></tr>
<tr><td>70</td></tr>
<tr><td>80</td><td rowspan="2">extensive damage</td><td rowspan="3">Grade 4</td><td rowspan="4">D4</td><td rowspan="3">Major</td></tr>
<tr><td>90</td><td rowspan="2">D5</td></tr>
<tr><td>100</td><td>complete damage</td><td>Grade 5</td><td>Partial collapse</td></tr>
</table>

Table 2: Detailed definition of building damage states in ~~GB17742-~~GB/T 17742-2008, China.

Damage state	Structural damage	Non-structural damage	Performance-based Description
D1	Negligible	Cracks only in *very few* non-structural components	No need to repair, instant use
D2	*Very few* components have visible cracks	Obvious cracks can be found	No need to repair or after slightly repairing, can be used directly
D3	*A few* components have slight cracks, *very few* have obvious cracks	*Most* components have serious damage	Certain repair work should be done before continued use
D4	*Most* components have serious damage, *a majority* have obvious cracks	*Most* components partially destroyed	The damage is difficult to repair
D5	*The majority* components have serious damage, the building structure is close to collapse or already collapsed	Non-structural components are *commonly* destroyed	To repair the building back to normal is impossible

Notes about qualifiers: "very few": <10%; "a few": 10%-50%; "most": 50%-70%; "majority": 70%-90%; "commonly": >90%.

Table 3: Divisions of seismic design level for Chinese buildings (modified after Lin et al., 2010).

Seismic Resistance Design Level (PGA)	Construction Age			
	before 1978	1979-1989	1989-2001	After 2001
IX (0.4g)	pre-code	moderate-code	high-code	high-code
VIII (0.3g)	pre-code	moderate-code	moderate-code	high-code
VIII (0.2g)	pre-code	low-code	moderate-code	high-code
VII (0.15g)	pre-code	low-code	low-code	moderate-code
VII (0.10g)	pre-code	pre-code	low-code	low-code
VI (0.05g)	pre-code	pre-code	pre-code	low-code

Table 4: The median fragility curve parameters regressed from empirical and analytical fragility data.

data_source	build_type	fort _level	damage_state	μ_{LS}	σ_{LS}	R^2
Empirical	masonry	A	LS1	6.926	1.539	0.99
			LS2	8.418	1.378	1
			LS3	9.412	1.189	1
			LS4	10.57	1.298	1
		B	LS1	7.658	1.393	0.98
			LS2	9.283	1.298	0.99
			LS3	10.43	1.505	0.99
			LS4	11.59	1.553	1
	RC	A	LS1	7.779	1.304	1
			LS2	9.057	0.9367	1
			LS3	9.893	0.9269	1
			LS4	10.95	0.9626	1
		B	LS1	8.135	1.191	1
			LS2	9.511	1.067	1
			LS3	10.54	0.8831	1
			LS4	11.77	1.075	1
Analytical	masonry	A	LS1	0.1732	0.7512	1
			LS2	0.33	0.7512	1
			LS3	0.5862	0.6383	0.99
			LS4	0.9416	0.4983	0.97
		B	LS1	0.3499	0.7573	1
			LS2	0.6743	0.8101	1
			LS3	1.281	0.8125	1
			LS4	2.595	0.8581	0.99
	RC	A	LS1	0.223	0.6615	**0.80**
			LS2	0.353	0.7699	**0.77**
			LS3	0.694	0.6111	**0.73**
			LS4	1.404	0.4818	0.98
		B	LS1	0.315	0.539	0.99
			LS2	0.46	0.5269	0.99
			LS3	0.811	0.346	0.95
			LS4	1.374	0.1763	0.91

*Note: "**fort_level**" **A** & **B** represent the pre/low/moderate-code and high-code seismic resistance level, respectively; "**damage_state**" LS1, LS2, LS3, LS4 represent the four damage limit states: slight, moderate, serious-, collapse, respectively; "μ_{LS}" and "σ_{LS}" are the regression parameters between intensity/PGA and the corresponding fragilities of each damage limit state; $\boldsymbol{R^2}$ indicates the fitness quality of the regressed median fragility curve, as plotted in Fig. 7 and Fig.8.

Table 5: The mean PGA values derived from intensity-PGA relations of "Masonry_A" based on the newly proposed approach (Sect. 5.4).

intensity	VI	VII	VIII	IX	X
PGA(g)	0.1	0.16	0.3	0.48	0.78

Table 6: The PGA ranges derived from more intensity-PGA relations (Sect. 5.5).

intensity	VI	VII	VIII	IX	X
PGA(g)	0.06-0.14	0.12-0.25	0.21-0.43	0.36-0.73	0.58-1.25

Table 7: The recommended intensity-PGA relations in China (~~GB17742-~~GB/T 17742-2008/1980).

intensity		VI	VII	VIII	IX	X
PGA (g)	mean	0.06	0.13	0.25	0.5	1.0
	range	0.05-0.09	0.09-0.18	0.18-0.35	0.35-0.7	0.7-1.4

Table 8: The latest intensity-PGA relation derived by traditional practice for mainland China (Ding, 2017).

intensity		VI	VII	VIII	IX
PGA (g)	mean	0.09	0.16	0.3	0.55
	range	0.06-0.12	0.09-0.22	0.22-0.41	0.41-0.75

Table B1: Statistics of fragility database for each damage limit state and each building type.

data source	build_type	intensity/ PGA(g)	original fragility number	fragility number after removing outliers				median value of each fragility dataset with truncated exceed. prob. ≥ 1%				standard deviation of each fragility dataset with truncated median exceed. prob. ≥ 1%			
				LS1	LS2	LS3	LS4	LS1	LS2	LS3	LS4	LS1	LS2	LS3	LS4
empirical	Masonry_A	6	29	28	28	28	28	0.30	0.06	0.01		0.13	0.04	0.01	
		7	29	29	26	26	27	0.47	0.14	0.04		0.21	0.08	0.04	
		8	29	29	29	25	26	0.78	0.40	0.11	0.03	0.20	0.27	0.07	0.02
		9	28	28	28	28	25	0.91	0.64	0.36	0.11	0.14	0.27	0.27	0.06
		10	28	27	26	28	28	0.99	0.90	0.69	0.33	0.05	0.15	0.26	0.22
	Masonry_B	6	21	21	21	21	21	0.15	0.02			0.09	0.02		
		7	21	21	20	18	18	0.26	0.08	0.02		0.21	0.10	0.03	
		8	21	21	21	21	18	0.66	0.17	0.07	0.01	0.30	0.24	0.16	0.01
		9	20	20	20	20	17	0.79	0.37	0.15	0.05	0.29	0.30	0.25	0.03
		10	20	20	20	20	20	0.96	0.74	0.39	0.15	0.24	0.31	0.30	0.22
	RC_A	6	24	23	22	19	24	0.12				0.07			
		7	24	23	23	22	24	0.25	0.02			0.14	0.05		
		8	26	26	24	24	23	0.57	0.12	0.02		0.19	0.12	0.06	
		9	20	20	20	19	18	0.82	0.48	0.17	0.02	0.14	0.17	0.08	0.02
		10	16	16	16	16	14	0.98	0.84	0.55	0.16	0.10	0.16	0.26	0.10
	RC_B	6	6	6	5	6	6	0.05				0.05			
		7	6	5	5	6	6	0.15	0.02			0.06	0.01		
		8	6	6	5	5	6	0.48	0.06			0.19	0.02		
		9	5	5	5	5	5	0.75	0.33	0.04		0.20	0.18	0.11	
		10	5	5	5	5	5	0.95	0.67	0.27	0.05	0.15	0.25	0.29	0.11
analytical	Masonry_A	0.1	6	6	6	5	6	0.22	0.06	0.02		0.14	0.06	0.01	
		0.2	6	6	6	6	6	0.60	0.25	0.08	0.02	0.15	0.13	0.06	0.01
		0.3	6	6	6	6	6	0.77	0.47	0.18	0.05	0.10	0.14	0.10	0.03
		0.4	6	6	6	6	6	0.86	0.60	0.29	0.09	0.07	0.14	0.14	0.07
		0.5	6	6	6	6	6	0.92	0.70	0.39	0.14	0.05	0.12	0.16	0.10
		0.6	6	6	6	6	6	0.95	0.77	0.50	0.20	0.04	0.10	0.16	0.13
		0.7	6	6	6	6	6	0.97	0.84	0.59	0.27	0.03	0.08	0.15	0.15
		0.8	6	6	6	6	6	0.98	0.88	0.66	0.34	0.02	0.07	0.15	0.17
		0.9	6	6	6	6	6	0.99	0.91	0.73	0.41	0.02	0.06	0.15	0.18
		1	6	6	6	6	6	0.99	0.94	0.78	0.47	0.02	0.05	0.14	0.19
		1.1	2	2	2	2	2	1.00	0.97	0.91	0.70	0.00	0.03	0.08	0.18
		1.2	2	2	2	2	2	1.00	0.98	0.93	0.74	0.00	0.03	0.05	0.16
	Masonry_B	0.1	6	6	6	6	6	0.04	0.02			0.05	0.01		
		0.2	6	6	6	6	5	0.21	0.05	0.01		0.14	0.05	0.01	
		0.3	6	6	6	6	5	0.43	0.14	0.04		0.19	0.09	0.02	
		0.4	6	6	6	6	6	0.59	0.25	0.08	0.01	0.21	0.14	0.05	0.01
		0.5	6	6	6	6	6	0.69	0.37	0.13	0.03	0.20	0.17	0.07	0.02
		0.6	6	6	6	6	6	0.76	0.45	0.18	0.05	0.17	0.18	0.09	0.03
		0.7	6	6	6	6	6	0.81	0.53	0.22	0.07	0.14	0.18	0.11	0.04
		0.8	6	5	6	6	6	0.86	0.59	0.28	0.09	0.06	0.17	0.13	0.06
		0.9	6	5	6	6	6	0.89	0.65	0.33	0.11	0.05	0.16	0.14	0.08
		1	6	5	6	6	6	0.91	0.70	0.39	0.13	0.04	0.15	0.15	0.10
		1.1	3	3	3	3	3	0.93	0.70	0.42	0.15	0.09	0.20	0.23	0.17
		1.2	3	3	3	3	3	0.95	0.75	0.48	0.19	0.08	0.19	0.24	0.19
	RC_A	0.1	20	18	18	20	17	0.07				0.07			
		0.2	20	20	18	19	20	0.42	0.13	0.01		0.32	0.12	0.03	
		0.3	22	22	22	21	20	0.72	0.45	0.05		0.29	0.35	0.09	
		0.4	20	20	20	20	18	0.78	0.48	0.10	0.02	0.26	0.36	0.21	0.02
		0.5	13	12	13	13	11	0.96	0.89	0.34	0.03	0.09	0.25	0.26	0.04
		0.6	22	22	22	22	19	0.93	0.82	0.33	0.05	0.30	0.41	0.32	0.05
		0.7	11	11	11	11	10	0.99	0.96	0.77	0.06	0.08	0.22	0.33	0.06
		0.8	17	17	17	17	15	0.88	0.64	0.37	0.15	0.38	0.36	0.37	0.08
		0.9	12	11	12	12	11	1.00	0.99	0.92	0.14	0.03	0.16	0.30	0.11
		1	16	16	16	16	15	0.91	0.70	0.41	0.25	0.49	0.38	0.34	0.13
		1.1	5	5	5	5	5	1.00	0.99	0.99	0.29	0.00	0.01	0.03	0.31
		1.2	14	14	14	14	14	0.61	0.68	0.67	0.39	0.47	0.43	0.34	0.27
	RC_B	0.1	9	8	9	9	9	0.02				0.02			
		0.2	9	8	7	9	9	0.18	0.04			0.28	0.02		
		0.3	11	11	11	10	11	0.50	0.22			0.35	0.32		
		0.4	9	9	9	8	9	0.65	0.37	0.04		0.25	0.33	0.04	
		0.5	9	9	9	8	8	0.79	0.57	0.08		0.21	0.31	0.08	
		0.6	11	11	11	10	10	0.93	0.75	0.20	0.02	0.18	0.30	0.10	0.01
		0.7	9	9	9	9	8	0.93	0.81	0.37	0.03	0.15	0.29	0.22	0.02
		0.8	8	8	8	8	7	0.91	0.79	0.45	0.03	0.12	0.26	0.29	0.02
		0.9	10	10	10	10	9	0.99	0.93	0.68	0.03	0.12	0.25	0.33	0.03
		1	7	7	7	7	7	0.94	0.83	0.52	0.05	0.09	0.22	0.33	0.04
		1.1	4	4	4	4	4	1.00	0.97	0.89	0.08	0.02	0.05	0.19	0.07
		1.2	6	5	5	5	6	1.00	0.99	0.98	0.23	0.00	0.01	0.06	0.12

Note: “origin fragility number” refers to the number of original fragilities collected for each damage limit state of each building type from previous studies; “fragility number after removing outliers” refers to the remaining fragilities after removing outliers using box-plot check method. Only intensity and PGA values with truncated exceedance probability ⩾1% for each damage limit state of each building type are given, since higher damage states can appear only for higher intensities or PGA values (see Sect. 5.2 for more details).

Table B2: Chinese Official Seismic Intensity Scale: ~~GB17742~~ ~~GB/T 17742~~-2008 (modified after CSIS, 2019).

Macro Intensity	Senses by people on the ground	Degree of building damage			Other damages	Horizontal motion on the ground	
		Building type	Damages	Average damage index		Peak acceleration(m/s^2)	Peak speed (m/s)
I	Insensible						
II	Sensible by very few still indoor people						
III	Sensible by a few still indoor people		Slight rattle of doors and windows		Slight swing of suspended objects		
IV	Sensible by most people indoors, a few people outdoors; a few wake up from sleep		Rattle of doors and windows		Obvious swing of suspended objects; vessels rattle		
V	Commonly sensible by people indoors, sensible by most people outdoors; most wake up from sleep		Noise from vibration of doors, windows, and building frames; falling of dusts, small cracks in plasters, falling of some roof tiles, bricks falling from a few roof-top chimneys		Rocking or flipping of unstable objects	0.31 (0.22-0.44)	0.03 (0.02-0.04)
VI	Most unable to stand stably, a few scared to running outdoors	A	A few have D3 damage	0-0.11	Cracks in river banks and soft soil; occasional burst of sand and water from saturated sand layers; cracks on some standalone chimneys	0.63 (0.45-0.89)	0.06 (0.05-0.09)
		B	Very few have D3 damage, a few have D2 damage, most are intact				
		C	Very few have D2 damage, the majority are intact	0-0.08			
VII	Majority scared to running outdoors, sensible by bicycle riders and people in moving motor vehicles	A	A few have D4 and/or D5 damage, most have D3 and/or D2 damage	0.09-0.31	Collapse of river banks; frequent burst of sand and water from saturated sand layers; many cracks in soft soils; moderate destruction of most standalone chimneys	1.25 (0.90-1.77)	0.13 (0.10-0.18)
		B	A few have D3 damage, most have D2 and/or D1 damage				
		C	A few have D3 and/or D2, most are intact	0.07-0.22			
VIII	Most swing about, difficult to walk	A	A few have D5 damage, most have D4 and/or D3 damage	0.29- 0.51	Cracks appear in hard dry soils; severe destruction of most standalone chimneys; tree tops break; death of people and cattle caused by building destruction	2.50 (1.78-3.53)	0.25 (0.19-0.35)
		B	Very few have D5 damage, most have D3 and/or D2 damage				
		C	A few have D4 and/or D3 damage, most have D2 damage	0.2-0.4			
IX	Moving people fall	A	Most have D4 and/or D5 damage	0.49-0.71	Many cracks in hard dry soils; possible cracks and dislocations in bedrock; frequent landslides and collapses; collapse of many standalone chimneys	5.00 (3.54-7.07)	0.50 (0.36-0.71)
		B	A few have D5 damage, most have D4 and/or D3 damage				
		C	A few have D5 and/or D4 damage, most have D3 and/or D2 damage	0.38-0.6			
X	Bicycle riders may fall; people in unstable state may fall away;	A	Commonly have D5 damage	0.69-0.91	Cracks in bedrock and earthquake fractures; destruction of bridge arches	10.00 (7.08-14.14)	1.00 (0.72-1.41)
		B	The majority have D5 damage				

	sense of being thrown up	C	Most have D5 and/or D4 damage	0.58-0.8	founded in bedrock; foundation damage or collapse of most standalone chimneys		
XI		A	Commonly have D5 damage	0.89–1.0	Earthquake fractures extend a long way; many bedrock cracks and landslides		
		B					
		C		0.78-1.0			
XII		A	Almost all have D5 damage	1.0	Drastic change in landscape, mountains, and rivers		
		B					
		C					

Notes about Qualifiers: "very few": <10%; "few": 10% - 50%; "most": 50% - 70%; "majority": 70% - 90%; "commonly": >90%.

Appendix C: Methodology in characterization of uncertainty transmission from empirical/analytical fragility database to intensity-PGA relation

The estimation of the uncertainty of the intensity-PGA relation (Eq. (5)) is not a standard procedure like regression analysis. We have fragility as function of intensity with an error on the fragility so that fragility is a random variable. It is also a random variable when derived as function of y = ln(PGA). We express this as

$$f(y) = g(y) + \varepsilon_g \quad \text{(C1)}$$

$$f(i) = h(i) + \varepsilon_h \quad \text{(C2)}$$

With i: intensity, y: ln(PGA), f: fragility.

ε_g is a normally distributed random variable with zero mean, standard deviation σ_g.

ε_h is a normally distributed random variable with zero mean, standard deviation σ_h.

$g(y)$ and $h(i)$ are non-linear functions that can be modelled as cumulative normal distributions in intensity and ln(PGA) as fragility ranges between 0 and 1. Under this condition equating the expectation values of the fragilities

$$E[f(y)] = E[f(i)], g(y) = h(i) \quad \text{(C3)}$$

Leads to a linear relation between ln(PGA) and intensity. Including uncertainties in this relation leads to the hypothesis

$$\ln(PGA) = y = \alpha + \beta \cdot i + \varepsilon_y \quad \text{(C4)}$$

ε_y is a normally distributed random variable with zero mean, standard deviation σ_y and this is the quantity we want to determine. Note that with this relation y became a random variable. Its expectation value is related to intensity via

$$E[y] = \bar{y} = \alpha + \beta \cdot i \quad \text{(C5)}$$

We ask the question: If the above relation holds and intensity is fixed what range of values for y is possible so that

$$f\big(y(i)\big) = f(i) \quad \text{(C6)}$$

holds. Inserting above expressions provides

$$g\big(\alpha + \beta \cdot i + \varepsilon_y\big) + \varepsilon_g = h(i) + \varepsilon_h \quad \text{(C7)}$$

If we assume that the error term is small, we can write:

$$g\big(\alpha + \beta \cdot i + \varepsilon_y\big) \approx g(\alpha + \beta \cdot i) + g'(\alpha + \beta \cdot i) \cdot \varepsilon_y \quad \text{(C8)}$$

$g'(\alpha + \beta \cdot i)$ is the slope of the g(y) curve and has the unit 1/ln(PGA). The value changes along the curve so that we replace it by an average value $\bar{g}'$. Then,

$$\varepsilon_y = \frac{1}{\bar{g}'}(\varepsilon_h - \varepsilon_g) \quad \text{(C9)}$$

and under the assumption of independence of the two random terms we get

$$\sigma_y = \frac{1}{\bar{g}'}\sqrt{\sigma_h^2 + \sigma_{\bar{g}}^2} \quad \text{(C10)}$$

In order to utilize this estimation scheme for our data we approximate $\bar{g}'$ by its value at the 0.5 value of the fragility function: $g(y_m) = 0.5$, so that $\bar{g}' = g'(y_m)$.When we do the estimates for each damage class and each building type we find the standard deviations for ln(PGA) according to the following table. The values do vary. A representative/average value appears to be 0.3.

Table B3: The standard deviation in intensity-PGA relation for each damage limit state of each building type.

Build_Type	LS1	LS2	LS3	LS4
Masonry_A	0.29	0.34	0.27	0.20
Masonry_B	0.48	0.49	0.44	0.25
RC_A	0.44	0.59	0.42	0.16
RC_B	0.27	0.32	0.24	0.05